

# Accepted Manuscript

Synthesis and evaluation of 2-(3-aryloreido)pyridines and 2-(3-aryloreido)pyrazines as potential modulators of A $\beta$ -induced mitochondrial dysfunction in Alzheimer's disease

Ahmed Elkamhawy, Jung-eun Park, Ahmed H.E. Hassan, Ae Nim Pae, Jiyoun Lee, Beoung-Geon Park, Eun Joo Roh

PII: S0223-5234(17)31079-6

DOI: [10.1016/j.ejmech.2017.12.045](https://doi.org/10.1016/j.ejmech.2017.12.045)

Reference: EJMECH 10023

To appear in: *European Journal of Medicinal Chemistry*

Received Date: 10 June 2017

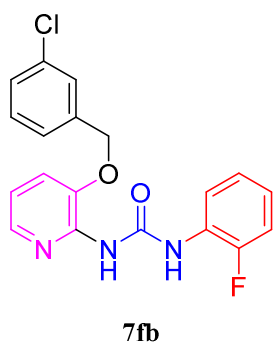
Revised Date: 9 November 2017

Accepted Date: 13 December 2017

Please cite this article as: A. Elkamhawy, J.-e. Park, A.H.E. Hassan, A.N. Pae, J. Lee, B.-G. Park, E.J. Roh, Synthesis and evaluation of 2-(3-aryloreido)pyridines and 2-(3-aryloreido)pyrazines as potential modulators of A $\beta$ -induced mitochondrial dysfunction in Alzheimer's disease, *European Journal of Medicinal Chemistry* (2018), doi: 10.1016/j.ejmech.2017.12.045.

This is a PDF file of an unedited manuscript that has been accepted for publication. As a service to our customers we are providing this early version of the manuscript. The manuscript will undergo copyediting, typesetting, and review of the resulting proof before it is published in its final form. Please note that during the production process errors may be discovered which could affect the content, and all legal disclaimers that apply to the journal pertain.



**Graphical Abstract:**

**JC-1 assay** = 11% increased g/r ratio

**MTT viability** = 115%

**ATP production** = 104%

**Protection against A $\beta$ -induced neurocytotoxicity** = 67%

**Protection against A $\beta$ -induced ATP suppression** = 43%

ACCEPTED MANUSCRIPT

# Synthesis and evaluation of 2-(3-aryllureido)pyridines and 2-(3-aryllureido)pyrazines as potential modulators of A $\beta$ -induced mitochondrial dysfunction in Alzheimer's disease

Ahmed Elkamhawy<sup>a,b,1</sup>, Jung-eun Park<sup>a,c,1</sup>, Ahmed H. E. Hassan<sup>d,e</sup>, Ae Nim Pae<sup>f,g</sup>, Jiyoun Lee<sup>h</sup>,  
Beoung-Geon Park<sup>f,i</sup>, Eun Joo Roh<sup>a,g,\*</sup>

<sup>a</sup> Chemical Kinomics Research Center, Korea Institute of Science and Technology (KIST), Seoul 02792, Republic of Korea

<sup>b</sup> Department of Pharmaceutical Organic Chemistry, Faculty of Pharmacy, Mansoura University, Mansoura 35516, Egypt

<sup>c</sup> Department of Chemistry, Sogang University, Seoul 04107, Republic of Korea

<sup>d</sup> Department of Medicinal Chemistry, Faculty of Pharmacy, Mansoura University, Mansoura 35516, Egypt

<sup>e</sup> Medicinal Chemistry Laboratory, Department of Pharmacy, College of Pharmacy, Kyung Hee University, Seoul 02447, Republic of Korea

<sup>f</sup> Convergence Research Center for Diagnosis, Treatment and Care System of Dementia, Korea Institute of Science and Technology (KIST), Seoul 02792, Republic of Korea

<sup>g</sup> Division of Bio-Medical Science & Technology, KIST School, Korea University of Science and Technology, Seoul, Republic of Korea

<sup>h</sup> Department of Global Medical Science, Sungshin Women's University, Seoul 142-732, Republic of Korea

<sup>i</sup> School of Life Sciences and Biotechnology, Korea University, Seoul 02792, Republic of Korea

## \*Corresponding author:

Eun Joo Roh (e-mail: r8636@kist.re.kr).

<sup>1</sup> Both authors contributed equally to this work

**Abstract**

A series of 2-(3-aryluroido)pyridines and 2-(3-benzylureido)pyridines were synthesized and evaluated as potential modulators for amyloid beta ( $A\beta$ )-induced mitochondrial dysfunction in Alzheimer's disease (AD). The blocking activities of forty one small molecules against  $A\beta$ -induced mitochondrial permeability transition pore (mPTP) opening were evaluated by JC-1 assay which measures the change of mitochondrial membrane potential ( $\Delta\Psi_m$ ). The inhibitory activity of twenty five compounds against  $A\beta$ -induced mPTP opening was superior to that of the standard cyclosporin A (CsA). Six hit compounds have been identified as likely safe in regards to mitochondrial and cellular safety and subjected to assessment for their protective effect against  $A\beta$ -induced deterioration of ATP production and cytotoxicity. Among them, compound **7fb** has been identified as a lead compound protecting neuronal cells against 67% of neurocytotoxicity and 43% of suppression of mitochondrial ATP production induced by 5  $\mu$ M concentrations of  $A\beta$ . Using CDocker algorithm, a molecular docking model presented a plausible binding mode for these compounds with cyclophilin D (CypD) receptor as a major component of mPTP. Hence, this report presents compound **7fb** as a new nonpeptidyl mPTP blocker which would be promising for further development of Alzheimer's disease (AD) therapeutics.

**Keywords:** Mitochondrial permeability transition pore (mPTP), Alzheimer's disease (AD),  $\beta$ -amyloid peptide ( $A\beta$ ), pyridyl-urea, molecular docking.

## 1. Introduction

Over the past decades, the presence of a mitochondrial channel involved in permeability transition, understanding its formation, regulation, and roles, has been a subject of debate and intense research [1-9]. Culminated data suggest that acute mitochondrial permeability transition pore (mPTP) opening is a physiologic process that contributes to the regulation and cycling of calcium in the mitochondria [9-11]. However, prolonged opening of mPTP results in loss of mitochondrial membrane potential, termination of ATP production, deterioration of homeostasis, swelling of mitochondria and eventually rupture of the outer mitochondrial membrane and release of cell death factors [12-15]. The detrimental sequences of prolonged mPTP opening have been correlated with several pathologies found in a wide range of diseases including cardiovascular, neurological, and hepatic diseases [16-26]. Inhibition of mPTP opening has been proved as a valid approach for cytoprotection against cell death in diseases characterized by excessive opening of mPTP [27-30].

The molecular structure of mPTP has been always a subject of controversy. Several elements have been suggested to be involved in mPTP formation; however, the exact structure is not certainly confirmed. The current model of mPTP involves dimers of  $F_0/F_1$  ATPase as the core unit of the pore; in addition to adenine nucleotide translocator (ANT) and inorganic phosphate carrier (PiC). According to this model, there are direct interactions of  $F_0/F_1$  ATPase dimer with CypD in the mitochondrial matrix, mitochondrial creatine kinase oligomers in intermembrane space, voltage dependent anion channel, Bcl-2-associated X protein and Bcl-2 homologous antagonist killer in the outer membrane. In addition, other regulatory elements exist including

mitochondrial translocator protein, protein kinase C epsilon and glycogen synthase kinase 3-beta [31].

Despite the debate over the molecular structure of mPTP, the role of cyclophilin D (CypD) in modulating mPTP opening is indubious [32, 33]. In fact, the suggestion of the presence of mPTP by Haworth and Hunter [34] was later confirmed by the discovery that inhibition of CypD by cyclosporin A (CsA) causes inhibition of transient potential [35, 36]. Although CsA is an effective mPTP inhibitor, it has also immunosuppressant activity which limits its therapeutic use as mPTP inhibitor [37]. In addition, being a polypeptide, its poor kinetics across blood brain barrier (BBB) results in low bioavailability to central nervous system neurons [38]. Efforts towards separation of immunosuppressant activity from cyclophilin inhibition activity afforded CsA analogs free from immunosuppressant activity. In addition to other side effects of such analogs, like NIM811 and UNIL025, they still suffer from poor penetration of BBB caused by their polypeptidic structure [39, 40]. Few reports are found in the literature documenting efforts to develop non-peptidic small molecule inhibitors of mPTP. Quinoxaline derivative **1** in Fig. 1, was described by Guo *et al.* as a selective agent for inhibition of CypD over cyclophilin A (CypA), albeit in micromolar activity [41]. To the best of our knowledge, there are no further reports of developing more potent or selective quinoxaline compounds as mPTP modulators. Furamide derivatives **2**, have been reported to possess inhibitory activity on calcium induced mitochondrial swelling *via* modulation of mPTP, however, at high micromolar concentration and low potency [42]. *N*-phenylbenzamide **3** has been found to maintain mitochondrial potential in models of calcium-induced mitochondrial permeability transition. However, they act on unknown biological target(s) [43]. The selective, safe, non-peptidic, bioavailable, small molecule

inhibitor sought for is still lacking. This situation stimulated our institute to initiate a discovery project aiming to find promising hit molecules as mPTP modulators. In the early stage of the project, screening of our institute chemical library using JC-1 assay resulted in identification of quinuclidinyl oxime ether **4** as a hit compound recovering the amyloid beta (A $\beta$ )-induced impairment of mitochondrial membrane potential [44]. Structural modifications of the hit compound afforded substituted pyrrolidinyl triazoles **5** as potential mPTP blockers [45]. It is known that 1,2,3-triazoles might act as a hydrogen bond acceptor, elicit  $\pi$ - $\pi$  stacking and/or contribute to dipole-dipole interactions. Considering this fact, we have reported the identification of a urea linked compound (**6**) as a promising lead compound recovering mitochondria from amyloid beta induced mPTP opening and membrane potential loss [46]. Moreover, it exerted a significant protection against amyloid beta induced mitochondrial and cellular toxicities.

< Please Insert Fig. 1. Here >

Investigation of the crystal structure of CsA-CypD complex (Fig. 2. pdb ID = 2Z6W) indicates a crucial role for hydrophobic interactions in addition to the known hydrogen bonding interactions [47]. These hydrophobic interactions include CsA's methylated valine residue (Mva11) within the critical main binding pocket (P1), CsA's methylated leucine residue side chain (Mle9) with a flat hydrophobic surface (S2) adjacent to pocket P1 and a neighboring Ala103 residue with side chain of 4-(2-butenyl)-4-methylthreonine residue (Bmt1) residue of CsA. The hydrogen bonding of CsA includes with Gln63 and Asn102 in the saddle region (S1) separating the main binding pocket P1 from a partially filled pocket (P2); hydrogen bonds with Arg55 and His126 at the edge

of the main binding pocket P1; and Trp121 in a flattened hydrophobic surface (S2) adjacent to the other side of the hydrophobic pocket P1.

< Please Insert Fig. 2. Here >

Considering the pivotal role of hydrophobic interactions with the flattened hydrophobic surface next to the main binding pocket, as well as, hydrogen bond bonding interactions, we anticipated that incorporation of planar aromatic moieties in place of the aliphatic cyclic amines moieties of compounds **4**, **5** and **6** while conserving the urea linker would result in enhanced hydrophobic interaction with the hydrophobic surface and would produce ligands with enhanced biological activities. The introduced aromatic moieties could be attached to the urea moiety through a methylene group or alternatively directly attached. Different mono or fused aromatic rings with different substitution patterns were considered in the target molecules (**7**). Moreover, assessment of the effect on the elicited biological activity by both of using different halogenation patterns of the benzyloxy ring, and isosteric replacement of pyridine with pyrazine on the elicited biological activity was planned.

< Please Insert Fig. 3. Here >

## 2. Results and discussion

### 2.1. Chemistry

Conciseness of chemical synthesis is a desirable sensible practice. The less number of synthetic steps, the more economic and efficient the synthetic process. Considering this point, the designed synthetic Scheme 1 for preparation of the target compounds (**7aa–7hc**) involved two synthetic

steps employing commercially available starting materials, 2-amino-3-hydroxypyridine (**8a**) or 2-amino-3-chloropyrazine (**8b**). While 3-(benzyloxy)pyridine-2-amine (**9a**) is commercially available, other 3-benzyloxy-2-pyridinamine derivatives (**9b–f**) were prepared *via* *O*-alkylation of 2-amino-3-hydroxypyridine (**8a**) with the appropriate benzyl bromide derivative in biphasic medium using tetra-*n*-butylammonium bromide as a phase transfer catalyst and sodium hydroxide as a base [46]. Meanwhile, nucleophilic aromatic substitution of 2-amino-3-chloropyrazine (**8b**) with appropriate phenylmethoxide anion generated from corresponding benzyl alcohol and sodium hydride yielded 3-benzyloxy-2-pyrazinamine derivatives (**9g** and **9h**). The target urea linked derivatives (**7aa–hc**) were obtained *via* addition reaction of the nucleophilic amino derivatives (**9a–h**) to the appropriate electrophilic aromatic isocyanate derivatives.

< Please Insert Scheme 1. Here >

## 2.2. Biological evaluation

### 2.2.1. JC-1 assay (Mitochondrial membrane potential assay)

Opening of mPTP leads to depolarization of the potential across the mitochondrial membrane. This loss of potential can be measured and quantified using a suitable indicator such as JC-1; a lipophilic fluorescent cationic dye. In mitochondria with conserved membrane potential, it forms aggregates eliciting characteristic red fluorescence. Upon loss of mitochondrial membrane, these aggregates dismantle into green fluorescent monomers. This behavior is dependent only on the mitochondrial membrane potential and is not affected by other factors such as mitochondrial size or shape, which renders the test highly specific. Accordingly, JC-1 assay can be used for evaluation of the effect of different molecules on the mitochondrial membrane potential *via*

measuring and quantification of the ratio of red to green fluorescence. In the course of the conducted test, mPTP opening was induced by amyloid beta ( $A\beta$ ) resulting in potential loss and shifting from red to green fluorescence. Doses of five micromolar concentrations were used to evaluate the capability of the tested compounds to block mPTP and recover the mitochondrial potential by measuring the decrement of green to red fluorescence. The results of the tested compounds are shown in Table 1. CsA was used as a standard, whereby, it lowered the green to red ratio to 46% of that of  $A\beta$  alone.

< Please Insert Table 1. Here >

Initially, four series of unsubstituted benzyloxy and 3-fluorobenzyloxy derivatives of pyridine and pyrazine containing compounds (**7aa–7dd**) were synthesized and evaluated using JC-1 assay. As shown in Fig. 4, the assay results revealed high efficiency for pyridine over pyrazine containing derivatives in reduction of the green to red fluorescence ratio. Most of pyridine derivatives exerted excellent lowering of green to red fluorescence more than that of standard CsA while the tested pyrazine compounds were ineffective in lowering the green to red fluorescence. With only 9% green to red fluorescence, pyridine derivative **7ca** was the most potent pyridine derivative in this four series. In comparison, the analogous pyrazine derivative **7da** was the only derivative showing significant activity, despite being weak.

< Please Insert Fig. 4. Here >

Based on these initial results, further four series of pyridine derivatives having different halogenation pattern on the benzyloxy moiety were prepared. Their JC-1 assay results are also presented in Table 1 and visualized in Fig. 5. Investigating collectively the activity data of the prepared pyridine derivatives, it can be concluded that, for the other aromatic ring linked to urea, the two fused rings (naphthyl derivatives) generally elicited weak or no efficacy as shown for compounds **7eg**, **7fh** and **7gg** (Fig. 5). Other compounds having single ring moieties linked to urea were generally more efficient in lowering the green to red fluorescence. The 2-fluorophenyl and 3-fluorophenyl urea derivatives were more efficient than the 3-chlorophenyl and 3,4-dichlorophenyl urea derivatives. However, the 3,4-dichlorophenyl urea derivative (**7fe**) was highly efficient in blocking A $\beta$ -induced mPTP opening, eliciting a very low increase in green to red fluorescence ratio. Considering the halogenation pattern on the benzyloxy ring, it can be generally concluded that fluorination or chlorination at position 3 afford more efficient compounds than chlorination at position 2 or 4. 3-Chlorobenzyloxy derivatives were generally more active as mPTP blockers than 3-fluorobenzyloxy analogs. Four highly efficient derivatives (**7fe**, **7fb**, **7fc** and **7fa**) eliciting lowering of the produced green to red fluorescence ratio to 15% or less were 3-chlorobenzyloxy derivatives, while one derivative was 3-fluorobenzyloxy (**7ca**), one was 4-chlorobenzyloxy derivative (**7gb**), and one was unsubstituted benzyloxy derivative (**7ab**).

< Please Insert Fig. 5. Here >

### 2.2.2. Assessment of effect on mitochondrial ATP production and neurocytotoxicity

Toxicity is a major cause for termination of drug discovery programs in preclinical, Phase I and Phase II. Therefore, it becomes imperative to assess toxicity early in drug discovery programs. Employing front toxicity assays would allow filtering out the likely toxic molecules; thus saving spent efforts and costs and minimizing the probability of molecules failure in later stages of development. Mitochondrial toxicity is a major concern for safety in drugs development. In addition to the fact that mitochondria are cell's energy plant, the recently proposed model of mitochondrial permeability transition pore suggested dimers of  $F_0/F_1$  ATPase as the core unit of the pore. Accordingly, it is crucial to assess effect of the promising prepared compounds on mitochondrial ATP production. The impact of a set of highly active compounds on ATP production was evaluated using hippocampal neuronal cell line after incubation for 7 hours with five micromolar concentrations of tested compound. As Table 2 shows, no decrement of ATP production was measured for all tested compounds while the standard piracetam elicited ATP production percent equal to 88%. This indicates absence of detrimental effects of the tested compounds on the vital mitochondrial energy production process. Next employed toxicity filter was set to exclude cytotoxic molecules. In addition to the fact that cytotoxicity is generally unwanted effect for development of safe drugs, it would also worsen degenerative diseases as in these disease patients already suffers from loss of function due to cell death. For assessment of cytotoxicity, MTT cell viability assay using hippocampal neuronal cell line HT-22 was employed to evaluate neurocytotoxicity of tested compounds. In the performed assay cells were incubated with 5  $\mu$ M concentrations of each tested compound for 24 hours. The results presented in Table 2 shows that almost all tested compounds have acceptable viability values comparable to the standard CsA (Table 2). Only one compound **7ee** showed significant lowering of cells viability and thus was excluded from further biological evaluation and testing.

< Please Insert Table 2. Here >

### 2.2.3. Protection against A $\beta$ -induced impairment of ATP production

In addition to A $\beta$ -induced loss of mitochondrial potential, deterioration of ATP synthesis is another major outcome of A $\beta$ -induced mitochondrial dysfunction. It is demanded that candidate molecules be also capable of lessening impairment of ATP production induced by A $\beta$ . The set of active compounds which elicited mPTP blocking activity better than CsA in JC-1 assay and passed through mitochondrial and cellular toxicity filters, were subjected for evaluation of their capacity to protect the cells against A $\beta$ -induced deterioration of ATP production employing a luciferase based cellular ATP assay in hippocampal neuronal cell line using piracetam as a reference standard. As presented in Table 3 and illustrated in Fig. 6, the level of ATP production in A $\beta$ -injured cells was considered as the base line having an arbitrary value of zero. The heights of bars represent the percent recovered ATP production. Thus a value of 100% equals to the value of ATP production in the vehicle treated cells. Using a dose of 5  $\mu$ M concentration, all tested compounds showed significant protection against A $\beta$ -suppression of ATP production, however, with variable capacities. Two compounds (**7ed** and **7fa**) were able to protect cells against almost all of the A $\beta$ -induced deterioration of ATP production (91% and 90% respectively). Another two compounds (**7ec** and **7fc**) elicited high capacity for maintaining mitochondrial ATP production (78% and 69% respectively). Among tested compounds, compounds **7ff** and **7fb** exhibited the lowest, however, significant capacity for protection against A $\beta$ -induced deterioration of ATP production (54% and 43% respectively). The culminated results of JC-1 assay, mitochondrial and cellular toxicity assays, in addition to protection against

A $\beta$ -suppressed production of ATP, indicated that tested compounds are likely safe molecules with potential capabilities to ameliorate A $\beta$ -induced mitochondrial dysfunction.

< Please Insert Table 3. Here >

< Please Insert Fig. 6. Here >

#### 2.2.4. Protection against A $\beta$ -induced neurocytotoxicity

Progressive neuronal cells death is the major problem manifested in neurodegenerative diseases. This neurocytotoxicity is a consequence of complex multiple mechanisms. An effective treatment should eventually be capable of protecting neuronal cells against this progressive cytotoxicity. Therefore, next to affirming that tested compounds elicited significant ability to reduce A $\beta$ -induced mitochondrial dysfunction, assessment of compounds ability to protect neuronal cells from A $\beta$ -induced neurocytotoxicity was performed employing hippocampal neuronal cell line and the results are presented in Table 3 and visualized in Fig. 6. In the figure, the viability level of A $\beta$ -treated cells was considered as the base line having an arbitrary value of zero. The heights of bars represent the percent protection from A $\beta$ -induced cytotoxicity of hippocampal neuronal cells recovery of ATP production. A value of 100% protection of A $\beta$ -induced cytotoxicity equals to the measured viability level of the vehicle treated cells. At a concentration of 5  $\mu$ M, compound **7fb** exhibited significantly high capacity to protect neuronal cells from A $\beta$ -induced cytotoxicity (inhibition of 67% of the cytotoxicity of 5  $\mu$ M concentrations of A $\beta$ ). In addition, compound **7fc** showed low, however, significant capacity to protect neuronal cells from A $\beta$ -induced cytotoxicity (inhibition of 38% of the neuronal cytotoxicity). The remaining evaluated compounds exhibited protective capacities lower or comparable to the

reference Piracetam. The culminated results of successively performed biological evaluation indicate that compound **7fb** could be a promising a lead compound possessing significant abilities to protect neuronal cells from A $\beta$ -induced mitochondrial dysfunctions and cells death.

### 2.2.5. Molecular docking

CypD, a cyclophilin family member in mitochondrial matrix, is a peptidyl prolyl *cis-trans* isomerase PPI that modulates mPTP opening and loss of membrane potential. CsA is a cyclic polypeptide that has been found to strongly bind to CypD blocking mPTP opening. Inspection of crystal structure of CypD-CsA complex (pdb ID = 2Z6W) discloses hydrophobic interactions as the major contributor in binding. A crucial hydrophobic binding pocket 1 formed by residues Met61, Ala101, Phe113, Leu122 and His126 is the binding site for the CsA's methylated valine residue (Mva11). Another less hydrophobic pocket (2), in which the CsA's  $\alpha$ -amino-butyric acid residue (Aba2) is interacting with Gln111 and Gly72, is located next to pocket 1. Pockets 1 and 2 are separated by a saddle formed of Gln63, Ala101, and Asn102. On the other side next to pocket 1, a flat hydrophobic surface formed of Phe60, Ile57 and Trp121, is located. This hydrophobic surface interacts with which the side chain of CsA's methylated leucine residue (Mle9). The side chain of 4-(2-butenyl)-4-methylthreonine residue (Bmt1) interacts hydrophobically with a nearby Ala103 residue. Hydrogen bonding interactions are found with amino acids Gln63 and Asn102 in the saddle region, Arg55 and His126 at the edge of pocket 1, and Trp121 in the flattened hydrophobic surface next to pocket 1.

A molecular modeling study was conducted to understand the difference in the tested compounds capabilities in blocking mPTP. Sets of the pyridine derivatives highly effective for mPTP

blocking (**7ab**, **7ac**, **7ca**, **7fa**, **7fb**, **7fc**, **7fe**, **7gb** and **7hb**), pyridine derivatives ineffective for mPTP blocking (**7ea**, **7fh**, **7gf** and **7hc**) and pyrazine derivatives (**7ba**, **7bb**, **7da**, **7db**, **7dc** and **7dd**) were docked into the reported crystal structure of human CypD (pdb ID = 2Z6W) after appropriate preparation of receptor and ligands. CDocker algorithm, which is a CHARMM force field based docking method implemented in Accelrys Discovery Studio 4.0, was used as a flexible ligand docking method to predict the binding mode of different ligands to CypD. This algorithm uses explicit all-atoms CHARMM force field calculations which give more accurate prediction of correct pose than grid-based algorithms. Refinements of the poses were done using *in situ* minimizations of the resulting poses. The binding energies and complexes energies were calculated. Selection of the most probable binding modes was based on these calculated energy terms.

Analysis of calculated binding modes revealed two general binding modes for this class of compounds with CypD. The first general binding mode is characterized by part of the ligand being buried into the hydrophobic pocket 1, which is binding site for methylated valine residue (Mva11) of CsA. The buried part of the molecule is in almost hydrophobic interactions with residues forming the pocket. This binding mode is generally favored by effective mPTP blockers. In the second general binding mode, the hydrophobic pocket is vacant while the ligand is docked above it. The second binding mode is more frequently encountered in ineffective mPTP blockers as the preferable binding mode.

The different binding modes for the effective mPTP blocker **7ab** are illustrated in Fig. 7. Out of twenty retrieved different poses, compound **7ab** showed nineteen poses belonging to general

binding mode 1. Only one pose was belonging to binding mode 2. The calculated energy terms for binding mode 2 were -55.99 kcal/mol for binding energy, -53.22 kcal/mol for total binding energy and -3075.61 kcal/mol for complex energy. Four binding poses belonging to binding mode 1 were superior to binding mode 2 in terms of binding energy, total binding energy and complex stability. This indicates the tendency for compound **7ab** to bind in mode 1 rather than mode 2.

< Please Insert Fig. 7. Here >

As shown in Fig. 7, three distinctive subtypes of binding modes can be identified under the general binding mode 1. In binding mode 1 subtype 1 (Fig. 7A), the eastern aromatic moiety is docked into the hydrophobic pocket 1. The overall best pose in terms of energy for compound **7ab** docked in this pose (-58.06 kcal/mol for binding energy, -56.36 kcal/mol for total binding energy and -3076.99 kcal/mol for complex energy) belongs to this subtype of binding mode.

Binding mode 1 subtype 2 (Fig. 7B) is characterized by pyridine ring docked into the hydrophobic pocket 1. This subtype of mode 1 was detected in ten poses out of the generated twenty poses for compound **7ab**. Despite the binding energy of the best pose of this subtype of binding mode 1 is slightly higher than best pose for subtype 1 (-58.23 kcal/mol for binding energy), the total binding energy and complex energy favors subtype 1 over this subtype (-53.61 kcal/mol for total binding energy and -3068.71 kcal/mol for complex energy). It is noted that poses belonging to this subtype showed rotation of the pyridine ring within the pocket resulting in different orientations of benzyloxy and eastern aromatic moiety groups.

In subtype 3 of binding mode 1 (Fig. 7C), the benzyloxy moiety of compound **7ab** is docked into the hydrophobic pocket 1. The calculated energy terms (-55.57 kcal/mol for binding energy, -50.26 kcal/mol for total binding energy and -3069.01 kcal/mol for complex energy) indicate that mode 1 subtype 3 is energetically much less favored than mode 2 and other mode 1 subtypes.

Binding mode 2 is illustrated in Fig. 7D. This mode, which has been detected only in one pose for compound **7ab**, is characterized by hydrophobic pocket 1 being unfilled. The ligand in this mode docked above the pocket. Considering all of previously mentioned binding modes in conjunction with their calculated energy terms, the potent activity of compound **7ab** can be attributed to dominating binding mode 1 subtype 1.

Compound **7ba** is shown in Fig. 8 as a representative example for ineffective compounds. The highest scoring binding modes were for binding mode 1 subtype 3 (Fig. 8A) and binding modes 2 (Fig. 8B). As mentioned previously, binding mode 2 contribution leads to ineffective mPTP blockers. In addition, inspection of binding mode 1 revealed high ligand energy for the docked conformations of compound **7ba** which would disfavor this binding mode. The calculated energy terms for the pose of compound **7ba** shown in Fig. 8A revealed high ligand energy for the docked pose (20.58 kcal/mol).

< Please Insert Fig. 8. Here >

### 3. Conclusion

In this study, a new series of *N*-benzyl and *N*-aryl-*N'*-heteroaryl urea derivatives was prepared and evaluated as protective agents against A $\beta$ -induced mitochondrial dysfunctions and neurocytotoxicity. Out of forty one prepared compounds, twenty five derivatives protected mitochondria more effectively than CsA from A $\beta$ -induced loss of mitochondrial membrane potential ( $\Delta\Psi_m$ ). It is noteworthy that these newly synthesized compounds, in contrast to quinoxaline derivatives **1**, furamide derivatives **2** and *N*-phenylbenzamide **3**, were evaluated in a model of A $\beta$ -induced loss of mitochondrial membrane potential which is more relevant to Alzheimer's disease while other compounds were evaluated in models of calcium-induced mitochondrial swelling which is non-relevant to Alzheimer's disease. In addition, these new compounds have elicited more efficient protective activity than quinuclidinyl oxime ether **4**, pyrrolidinyl triazoles **5**, and urea linked compound (**6**). Moreover, evaluation of their protection of neuronal cells from A $\beta$ -induced deterioration of ATP production and cytotoxicity identified compound **7fb** as a lead compound protecting neuronal cells against 67% of neurocytotoxicity and 43% of impairment of mitochondrial ATP production induced by 5  $\mu$ M concentrations of A $\beta$ . Furthermore, *in silico* docking simulations provided rational explanation of the observed mPTP blocking activity of this series. In summary, this study presents 2-(3-aryluroido)pyridines and 2-(3-aryluroido)pyrazines as new modulators of A $\beta$ -induced mitochondrial dysfunctions and identified compound **7fb** as a promising lead compound for development of new AD therapeutics.

## 4. Experimental

### 4.1. Chemistry

General: All reactions and manipulations were performed in nitrogen atmosphere using standard Schlenk techniques. The reaction solvents purchased from Aldrich Co., TCI and Alfa and used without any other purification. 3-(Benzyloxy)pyridin-2-amine **9a** has been purchased from Alfa Aesar Co. The NMR spectra were obtained on Bruker Avance 300 or 400. <sup>1</sup>H NMR spectra were referenced to tetramethylsilane ( $\delta = 0.00$  ppm) as an internal standard and are reported as follows: chemical shift, multiplicity (br = broad, s = singlet, d = doublet, t = triplet, dd = doublet of doublet, m = multiplet). Column chromatography was performed on Merck Silica Gel 60 (230–400 mesh) and eluting solvents for all of these chromatographic methods are noted as appropriated-mixed solvent with given volume-to-volume ratios. TLC was carried out using glass sheets pre-coated with silica gel 60 F<sub>254</sub> purchased by Merk. The purity of samples was determined by analytical HPLC using a Water ACQUITY UPLC (CORTECS™) with C18 column (2.1 mm x 100 mm; 1.6  $\mu$ m) at temperature 40 °C. HPLC data were recorded using parameters as follows: 0.1% formic acid in water and 0.1% formic acid in methanol and flow rate of 0.3 mL/min. For more details, see supplementary file. High-resolution spectra were performed on Waters ACQUITY UPLC BEH C18 1.7 $\mu$ -Q-TOF SYNAPT G2-Si High Definition Mass Spectrometry.

#### 4.1.1. 3-(Benzyloxy)pyridin-2-amine derivatives (**9b–f**).

Compounds **9b–9f** have been synthesized as reported by our group in a previous work [46].

#### 4.1.2. General procedure of 3-(benzyloxy)pyrazin-2-amine derivatives (**9g** and **9h**).

Sodium hydride (60% in mineral oil, 0.04 g, 1 mmol) was added to a stirred solution of benzyl alcohol derivative (1 mmol) in anhydrous *N,N*-dimethylformamide (3 mL of DMF) at room

temperature and stirring was continued for 1 h. 2-Amino-3-chloropyrazine (**8b**, 0.13 g, 1 mmol) was added to the reaction mixture and the reaction mixture was stirred at 100 °C for 15 h. After cooling, the solvent was evaporated and the residue was partitioned between water and dichloromethane. The organic layer was dried over sodium sulfate anhydrous, filtered, and concentrated. The residue was purified by column chromatography (SiO<sub>2</sub>, EA/*n*-Hex = 1/5).

### 3-(Benzyloxy)pyrazin-2-amine (**9g**)

Yellow solid, yield: 53.8%, <sup>1</sup>H NMR (400 MHz, CDCl<sub>3</sub>) δ = 5.45 (2H, s, OCH<sub>2</sub>Ph), 6.20 (2H, br, NH<sub>2</sub>), 7.38-7.48 (7H, m, ArH). Reported [48, 49].

### 3-(3-Fluorobenzyloxy)pyrazin-2-amine (**9h**)

Light orange solid, yield: 75.6%, <sup>1</sup>H NMR (400 MHz, DMSO-*d*<sub>6</sub>) δ = 5.39 (2H, s, OCH<sub>2</sub>Ph), 6.36 (2H, br, NH<sub>2</sub>), 7.14 (1H, td, *J* = 2.6 Hz, 9.0 Hz, ArH), 7.25 (1H, d, *J* = 3.1 Hz, ArH), 7.32 (1H, d, *J* = 7.6 Hz, ArH), 7.37-7.44 (2H, m, ArH), 7.49 (1H, d, *J* = 3.1 Hz, ArH).

#### 4.1.3. General procedure of final urea compounds (**7aa–7hc**)

2-Amino-3-benzyloxy pyridine or pyrazine derivative (2.5 mmol) was dissolved in dry THF (10 mL), isocyanate derivative (3.0 mmol) was added to the reaction mixture. The reaction was refluxed for 3–6 h. After cooling, the reaction mixture was evaporated and the residue was purified by solidification with cold methanol and filtered to give the target compounds.

### 1-(3-(Benzyloxy)pyridin-2-yl)-3-(2-fluorophenyl)urea (**7aa**)

White solid, yield: 91.1%, mp: 133.4-134.1 °C, HPLC purity: 7.21 min, 100%, <sup>1</sup>H NMR (400 MHz, CDCl<sub>3</sub>) δ = 5.13 (2H, s, OCH<sub>2</sub>Ph), 6.88 (1H, dd, *J* = 5.1 Hz, 8.0 Hz, ArH), 6.99-7.01 (1H, m, ArH), 7.07-7.16 (3H, m, ArH), 7.38-7.43 (5H, m, ArH), 7.56 (1H, s, NH), 7.88 (1H, dd, *J* = 1.2 Hz, 5.1 Hz, ArH), 8.30-8.35 (1H, m, ArH), 12.23 (1H, s, NH). <sup>13</sup>C NMR (100.6 MHz, CDCl<sub>3</sub>) δ = 70.92, 114.74 (*J*<sub>C-F</sub> = 18.5 Hz), 117.03, 118.04, 121.72, 123.20 (*J*<sub>C-F</sub> = 7.4 Hz), 124.41, 127.32, 127.83, 128.78, 128.94, 135.07, 137.12, 141.44, 143.55, 152.19, 152.97 (*J*<sub>C-F</sub> = 206.5 Hz). HRMS (ES<sup>+</sup>): *m/z* calculated for C<sub>19</sub>H<sub>16</sub>FN<sub>3</sub>O<sub>2</sub>: 338.1305 [M+H]<sup>+</sup>. Found 338.1335.

#### **1-(3-(Benzyloxy)pyridin-2-yl)-3-(3-fluorophenyl)urea (7ab)**

White solid, yield: 92.9%, mp: 122.8-123.5 °C, HPLC purity: 8.12 min, 100%, <sup>1</sup>H NMR (400 MHz, CDCl<sub>3</sub>) δ = 5.13 (2H, s, OCH<sub>2</sub>Ph), 6.74-6.77 (1H, m, ArH), 6.89 (1H, dd, *J* = 5.1 Hz, 8.0 Hz, ArH), 7.15 (1H, dd, *J* = 1.1 Hz, 8.0 Hz, ArH), 7.25-7.27 (m, 1H, ArH), 7.38-7.43 (5H, m, ArH), 7.27 (1H, s, NH), 7.50-7.55 (2H, m, ArH), 7.86 (1H, dd, *J* = 1.1 Hz, 5.1 Hz, ArH), 12.0 (1H, s, NH). <sup>13</sup>C NMR (100.6 MHz, CDCl<sub>3</sub>) δ = 70.92, 99.13, 107.43 (*J*<sub>C-F</sub> = 26.0 Hz), 109.93 (*J*<sub>C-F</sub> = 21.3 Hz), 115.40, 117.03, 118.09, 127.83, 128.82, 128.96, 129.83, 134.99, 136.92, 141.55, 143.67, 152.14, 152.92 (*J*<sub>C-F</sub> = 206.6 Hz). HRMS (ES<sup>+</sup>): *m/z* calculated for C<sub>19</sub>H<sub>16</sub>FN<sub>3</sub>O<sub>2</sub>: 338.1305 [M+H]<sup>+</sup>. Found 338.1382.

#### **1-(3-(Benzyloxy)pyridin-2-yl)-3-(3,4-dichlorophenyl)urea (7ac)**

White solid, yield: 83.7%, mp: 134.4-135.0 °C, HPLC purity: 7.61 min, 98.50%, <sup>1</sup>H NMR (400 MHz, CDCl<sub>3</sub>) δ = 5.13 (2H, s, OCH<sub>2</sub>Ph), 6.91 (1H, dd, *J* = 5.1 Hz, 8.0 Hz, ArH), 7.17 (1H, dd, *J* = 1.2 Hz, 8.0 Hz, ArH), 7.36 (1H, d, *J* = 8.8 Hz, ArH), 7.38-7.42 (5H, m, ArH), 7.47 (1H, dd, *J* = 2.5 Hz, 8.8 Hz, ArH), 7.54 (1H, s, NH), 7.80 (1H, d, *J* = 2.5 Hz, ArH), 7.86 (1H, dd, *J* = 1.2 Hz,

5.1 Hz, ArH), 12.04 (1H, s, NH).  $^{13}\text{C}$  NMR (100.6 MHz,  $\text{CDCl}_3$ )  $\delta$  = 70.95, 117.21, 118.21, 119.34, 121.57, 126.26, 127.83, 128.85, 128.97, 130.37, 132.55, 134.93, 136.88, 138.25, 141.58, 143.49, 152.04. HRMS ( $\text{ES}^+$ ):  $m/z$  calculated for  $\text{C}_{19}\text{H}_{15}\text{Cl}_2\text{N}_3\text{O}_2$ : 388.0619  $[\text{M}+\text{H}]^+$ . Found 388.0638.

**1-(3-(Benzyloxy)pyrazin-2-yl)-3-(2-fluorophenyl)urea (7ba)**

White solid, yield: 69.4%, mp: 159.9-163.4 °C, HPLC purity: 7.38 min, 100%,  $^1\text{H}$  NMR (400 MHz,  $\text{CDCl}_3$ )  $\delta$  = 5.38 (2H, s,  $\text{OCH}_2\text{Ph}$ ), 6.96-7.09 (3H, m, Ph), 7.32-7.40 (5H, m, ArH), 7.43 (1H, s, NH), 7.67 (1H, d,  $J$  = 3.1 Hz, ArH), 7.72 (1H, d,  $J$  = 3.1 Hz, ArH), 8.21-8.23 (1H, m, ArH), 11.56 (1H, s, NH).  $^{13}\text{C}$  NMR (100.6 MHz,  $\text{CDCl}_3$ )  $\delta$  = 69.00, 114.82 ( $J_{\text{C-F}}$  = 18.9 Hz), 121.84, 123.77 ( $J_{\text{C-F}}$  = 7.3 Hz), 124.48, 128.72, 131.63, 132.60, 135.32, 139.24, 148.02, 151.47, 163.02 ( $J_{\text{C-F}}$  = 287.5 Hz). HRMS ( $\text{ES}^+$ ):  $m/z$  calculated for  $\text{C}_{18}\text{H}_{15}\text{FN}_4\text{O}_2$ : 339.1857  $[\text{M}+\text{H}]^+$ . Found 339.1277.

**1-(3-(Benzyloxy)pyrazin-2-yl)-3-(3-fluorophenyl)urea (7bb)**

White solid, yield: 76.8%, mp: 134.4-134.8 °C, HPLC purity: 7.30 min, 97.91%,  $^1\text{H}$  NMR (400 MHz,  $\text{DMSO}-d_6$ )  $\delta$  = 5.47 (2H, s,  $\text{OCH}_2\text{Ph}$ ), 6.86-6.88 (1H, m, ArH), 7.26-7.41 (5H, m, ArH), 7.53-7.60 (3H, m, ArH), 7.83 (1H, d,  $J$  = 3.0 Hz, ArH), 7.93 (1H, d,  $J$  = 3.0 Hz, ArH), 9.00 (1H, s, NH), 11.01 (1H, s, NH).  $^{13}\text{C}$  NMR (100.6 MHz,  $\text{CDCl}_3$ )  $\delta$  = 70.04, 107.61 ( $J_{\text{C-F}}$  = 25.9 Hz), 110.46 ( $J_{\text{C-F}}$  = 21.2 Hz), 115.51, 128.75, 129.97 ( $J_{\text{C-F}}$  = 9.2 Hz), 131.97, 132.60, 135.26, 139.32, 139.58, 148.12, 151.42, 163.39 ( $J_{\text{C-F}}$  = 287.8 Hz). HRMS ( $\text{ES}^+$ ):  $m/z$  calculated for  $\text{C}_{18}\text{H}_{15}\text{FN}_4\text{O}_2$ : 339.1857  $[\text{M}+\text{H}]^+$ . Found 339.1269.

**1-Benzyl-3-(3-(3-fluorobenzyloxy)pyridin-2-yl)urea (7ca)**

White solid, yield: 74.4%, mp: 90.6-91.8 °C, HPLC purity: 6.80 min, 99.47%, <sup>1</sup>H NMR (400 MHz, CDCl<sub>3</sub>) δ = 4.62 (2H, d, *J* = 5.8 Hz, OCH<sub>2</sub>Ph), 5.09 (2H, s, OCH<sub>2</sub>Ph), 6.79 (1H, dd, *J* = 5.1 Hz, 8.0 Hz, ArH), 7.05 (1H, dd, *J* = 1.3 Hz, 8.0 Hz, ArH), 7.07-7.10 (2H, m, ArH), 7.17 (1H, d, *J* = 7.5 Hz, ArH), 7.26-7.27 (1H, m, ArH), 7.31-7.39 (5H, m, ArH), 7.45 (1H, s, NH), 7.74 (1H, dd, *J* = 1.3 Hz, 5.1 Hz, ArH), 9.90 (1H, s, NH). <sup>13</sup>C NMR (100.6 MHz, CDCl<sub>3</sub>) δ = 43.75, 69.95, 114.61 (*J*<sub>C-F</sub> = 22.0 Hz), 115.66 (*J*<sub>C-F</sub> = 20.8 Hz), 116.38, 117.62, 123.14, 127.05, 127.33, 128.55, 130.58 (*J*<sub>C-F</sub> = 8.1 Hz), 137.43, 137.67, 141.07, 144.16, 155.08, 163.00 (*J*<sub>C-F</sub> = 245.9 Hz). HRMS (ES<sup>+</sup>): *m/z* calculated for C<sub>20</sub>H<sub>18</sub>FN<sub>3</sub>O<sub>2</sub>: 352.1461 [M+H]<sup>+</sup>. Found 352.1489.

**1-(3-(3-Fluorobenzyloxy)pyridin-2-yl)-3-phenylurea (7cb)**

White solid, yield: 78.2%, mp: 97.4-100.7 °C, HPLC purity: 6.98 min, 96.84%, <sup>1</sup>H NMR (400 MHz, CDCl<sub>3</sub>) δ = 5.12 (2H, s, OCH<sub>2</sub>Ph), 6.87 (1H, dd, *J* = 5.1 Hz, 8.0 Hz, ArH), 7.06-7.12 (4H, m, ArH), 7.19 (1H, d, *J* = 7.7 Hz, ArH), 7.32-7.42 (3H, m, ArH), 7.49 (1H, brs, NH), 7.61 (2H, d, *J* = 7.5 Hz, ArH), 7.86 (1H, dd, *J* = 1.2 Hz, 5.1 Hz, ArH), 11.82 (1H, s, NH). <sup>13</sup>C NMR (100.6 MHz, DMSO-*d*<sub>6</sub>) δ = 69.08, 114.66 (*J*<sub>C-F</sub> = 22.2 Hz), 114.88 (*J*<sub>C-F</sub> = 21.2 Hz), 117.58, 118.16, 119.33, 119.67, 122.86, 123.78, 128.73, 128.86, 130.43 (*J*<sub>C-F</sub> = 8.1 Hz), 137.08, 138.68, 138.95 (*J*<sub>C-F</sub> = 7.5 Hz), 141.49, 143.28, 152.52, 162.22 (*J*<sub>C-F</sub> = 242.3 Hz). HRMS (ES<sup>+</sup>): *m/z* calculated for C<sub>19</sub>H<sub>16</sub>FN<sub>3</sub>O<sub>2</sub>: 338.1305 [M+H]<sup>+</sup>. Found 338.1328.

**1-(3-(3-Fluorobenzyloxy)pyridin-2-yl)-3-(2-fluorophenyl)urea (7cc)**

White solid, yield: 71.7%, mp: 118.8-119.3 °C, HPLC purity: 7.19 min, 99.35%, <sup>1</sup>H NMR (400 MHz, CDCl<sub>3</sub>) δ = 5.13 (2H, s, OCH<sub>2</sub>Ph), 6.74-6.77 (1H, m, ArH), 6.89 (1H, dd, *J* = 5.1 Hz, 8.0

Hz, ArH), 7.06-7.13 (3H, m, ArH), 7.18 (1H, d,  $J = 7.7$  Hz, ArH), 7.27-7.28 (2H, m, ArH), 7.37-7.41 (1H, m, ArH), 7.51 (1H, m, NH), 7.52-7.56 (1H, m, ArH), 7.87 (1H, dd,  $J = 1.2$  Hz, 5.1 Hz, ArH), 11.98 (1H, s, NH).  $^{13}\text{C}$  NMR (100.6 MHz,  $\text{CDCl}_3$ )  $\delta = 70.06, 114.65$  ( $J_{\text{C-F}} = 22.0$  Hz), 114.75 ( $J_{\text{C-F}} = 18.8$  Hz), 115.74 ( $J_{\text{C-F}} = 20.9$  Hz), 117.01, 118.08, 121.74, 123.21, 123.29, 124.45, 127.27, 137.41, 141.17, 143.52, 152.12, 152.97 ( $J_{\text{C-F}} = 242.4$  Hz), 163.02 ( $J_{\text{C-F}} = 245.9$  Hz). HRMS ( $\text{ES}^+$ ):  $m/z$  calculated for  $\text{C}_{19}\text{H}_{15}\text{F}_2\text{N}_3\text{O}_2$ : 356.1210  $[\text{M}+\text{H}]^+$ . Found 356.1231.

### 1-(3-(3-Fluorobenzyloxy)pyridin-2-yl)-3-(3-fluorophenyl)urea (7cd)

White solid, yield: 73.7%, mp: 134.2-135.2 °C, HPLC purity: 7.08 min, 99.02%,  $^1\text{H}$  NMR (400 MHz,  $\text{CDCl}_3$ )  $\delta = 5.13$  (2H, s,  $\text{OCH}_2\text{Ph}$ ), 6.88 (1H, dd,  $J = 5.1$  Hz, 8.0 Hz, ArH), 7.00-7.02 (1H, m, ArH), 7.06-7.11 (5H, m, ArH), 7.14 (1H, d,  $J = 7.92$  Hz, ArH), 7.37-7.41 (1H, m, ArH), 7.54 (1H, s, NH), 7.90 (1H, dd,  $J = 1.2$  Hz, 5.1 Hz, ArH), 8.30-8.35 (1H, m, ArH), 12.20 (1H, s, NH).  $^{13}\text{C}$  NMR (100.6 MHz,  $\text{CDCl}_3$ )  $\delta = 70.10, 99.14, 107.42$  ( $J_{\text{C-F}} = 25.9$  Hz), 109.96 ( $J_{\text{C-F}} = 21.2$  Hz), 114.65 ( $J_{\text{C-F}} = 22.0$  Hz), 115.41, 115.77 ( $J_{\text{C-F}} = 20.9$  Hz), 117.03, 118.12, 123.20, 129.88 ( $J_{\text{C-F}} = 9.4$  Hz), 130.65 ( $J_{\text{C-F}} = 8.1$  Hz), 137.21, 137.50, 140.20 ( $J_{\text{C-F}} = 10.6$  Hz), 141.27, 143.61, 152.07, 163.14 ( $J_{\text{C-F}} = 242.9$  Hz). HRMS ( $\text{ES}^+$ ):  $m/z$  calculated for  $\text{C}_{19}\text{H}_{15}\text{F}_2\text{N}_3\text{O}_2$ : 356.1210  $[\text{M}+\text{H}]^+$ . Found 356.1230.

### 1-(3-(3-Fluorobenzyloxy)pyridin-2-yl)-3-(3,4-dichlorophenyl)urea (7ce)

White solid, yield: 74.6%, mp: 141.8-142.5 °C, HPLC purity: 7.60 min, 92.91%,  $^1\text{H}$  NMR (400 MHz,  $\text{CDCl}_3$ )  $\delta = 5.13$  (2H, s,  $\text{OCH}_2\text{Ph}$ ), 6.91 (1H, dd,  $J = 5.1$  Hz, 8.0 Hz, ArH), 7.08-7.11 (2H, m, ArH), 7.13 (1H, dd,  $J = 1.3$  Hz, 5.1 Hz, ArH), 7.18 (1H, d,  $J = 7.8$  Hz, ArH), 7.36-7.40 (2H, m, ArH), 7.47 (1H, dd,  $J = 2.5$  Hz, 8.8 Hz, ArH), 7.52 (1H, s, NH), 7.80 (1H, d,  $J = 2.5$  Hz, ArH),

7.87 (1H, dd,  $J = 1.3$  Hz, 5.1 Hz, ArH), 12.01 (1H, s, NH).  $^{13}\text{C}$  NMR (100.6 MHz,  $\text{CDCl}_3$ )  $\delta =$  70.14, 114.66 ( $J_{\text{C-F}} = 22.3$  Hz), 115.81 ( $J_{\text{C-F}} = 20.9$  Hz), 117.18, 118.23, 119.35, 121.58, 123.19, 126.32, 130.38, 130.67 ( $J_{\text{C-F}} = 8.3$  Hz), 137.18, 137.37, 138.20, 141.30, 143.47, 151.98, 162.97 ( $J_{\text{C-F}} = 245.9$  Hz). HRMS ( $\text{ES}^+$ ):  $m/z$  calculated for  $\text{C}_{19}\text{H}_{14}\text{Cl}_2\text{FN}_3\text{O}_2$ : 406.0525  $[\text{M}+\text{H}]^+$ . Found 406.0552.

### 1-(3-(3-Fluorobenzyloxy)pyridin-2-yl)-3-(4-methylphenyl)urea (7cf)

White solid, yield: 72.2%, mp: 136.5-137.1 °C, HPLC purity: 7.19 min, 98.50%,  $^1\text{H}$  NMR (400 MHz,  $\text{CDCl}_3$ )  $\delta =$  2.32 (3H, s,  $\text{CH}_3$ ), 5.12 (2H, s,  $\text{OCH}_2\text{Ph}$ ), 6.86 (1H, dd,  $J = 5.1$  Hz, 8.0 Hz, ArH), 7.08-7.09 (3H, m, ArH), 7.12 (2H, m, ArH), 7.18 (1H, m, ArH), 7.37-7.39 (1H, m, ArH), 7.48 (3H, m, ArH+NH), 7.86 (1H, dd,  $J = 1.3$  Hz, 5.1 Hz, ArH), 11.71 (1H, s, NH).  $^{13}\text{C}$  NMR (100.6 MHz,  $\text{CDCl}_3$ )  $\delta =$  20.85, 70.04, 114.63 ( $J_{\text{C-F}} = 22.0$  Hz), 115.71 ( $J_{\text{C-F}} = 20.8$  Hz), 116.68, 117.90, 123.18, 129.44, 130.61 ( $J_{\text{C-F}} = 8.1$  Hz), 132.98, 135.88, 137.27, 137.62, 141.20, 144.89, 152.32, 163.02 ( $J_{\text{C-F}} = 246.0$  Hz). HRMS ( $\text{ES}^+$ ):  $m/z$  calculated for  $\text{C}_{20}\text{H}_{18}\text{FN}_3\text{O}_2$ : 352.1461  $[\text{M}+\text{H}]^+$ . Found 352.1483.

### 1-(3-(3-Fluorobenzyloxy)pyridin-2-yl)-3-(4-trifluoromethylphenyl)urea (7cg)

White solid, yield: 85.4%, mp: 156.5-157.3 °C, HPLC purity: 7.39 min, 93.73%,  $^1\text{H}$  NMR (400 MHz,  $\text{CDCl}_3$ )  $\delta =$  5.29 (2H, s,  $\text{OCH}_2\text{Ph}$ ), 6.92 (1H, dd,  $J = 5.5$  Hz, 8.0 Hz, ArH), 7.06-7.15 (3H, m, ArH), 7.19 (1H, d,  $J = 7.6$  Hz, ArH), 7.37-7.42 (1H, m, ArH), 7.55 (1H, s, NH), 7.58 (2H, d,  $J = 8.4$  Hz, ArH), 7.73 (2H, d,  $J = 8.4$  Hz, ArH), 7.89 (1H, dd,  $J = 1.2$  Hz,  $J = 5.2$  Hz, ArH), 12.13 (1H, s, NH). HRMS ( $\text{ES}^+$ ):  $m/z$  calculated for  $\text{C}_{20}\text{H}_{15}\text{F}_4\text{N}_3\text{O}_2$ : 428.0998  $[\text{M}+\text{Na}]^+$ . Found 428.0990.

**1-Benzyl-3-(3-(3-fluorobenzyloxy)pyrazin-2-yl)urea (7da)**

White solid, yield: 51.7%, mp: 121.7-121.4 °C, HPLC purity: 7.08 min, 96.93%, <sup>1</sup>H NMR (400 MHz, DMSO-*d*<sub>6</sub>) δ = 4.47 (2H, d, *J* = 6.0 Hz, OCH<sub>2</sub>Ph), 5.45 (2H, s, OCH<sub>2</sub>Ph), 7.15-7.17 (1H, m, ArH), 7.24-7.26 (1H, m, ArH), 7.32-7.37 (5H, m, ArH), 7.40-7.48 (2H, m, ArH), 7.73 (1H, d, *J* = 3.0 Hz, ArH), 7.80 (1H, d, *J* = 3.0 Hz, ArH), 8.69 (1H, s, NH), 9.27 (1H, s, NH). <sup>13</sup>C NMR (100.6 MHz, CDCl<sub>3</sub>) δ = 43.88, 67.89, 115.43 (*J*<sub>C-F</sub> = 21.7 Hz), 115.54 (*J*<sub>C-F</sub> = 20.9 Hz), 124.02, 127.26, 127.37, 128.63, 130.32 (*J*<sub>C-F</sub> = 8.1 Hz), 131.90 (*J*<sub>C-F</sub> = 4.8 Hz), 137.93, 138.80, 139.77, 147.64, 154.34, 162.88 (*J*<sub>C-F</sub> = 242.2 Hz). HRMS (ES<sup>+</sup>): *m/z* calculated for C<sub>19</sub>H<sub>17</sub>FN<sub>4</sub>O<sub>2</sub>: 353.1414 [M+H]<sup>+</sup>. Found 353.1491.

**1-(3-(3-Fluorobenzyloxy)pyrazin-2-yl)-3-(3-fluorophenyl)urea (7db)**

White solid, yield: 82.5%, mp: 152.3-153.4 °C, HPLC purity: 7.24 min, 100%, <sup>1</sup>H NMR (400 MHz, DMSO-*d*<sub>6</sub>) δ = 5.48 (2H, s, OCH<sub>2</sub>Ph), 6.87-6.90 (1H, m, ArH), 7.14-7.16 (1H, m, ArH), 7.28-7.49 (5H, m, ArH), 7.59 (1H, d, *J* = 11.9 Hz, ArH), 7.84 (1H, d, *J* = 3.0 Hz, ArH), 7.95 (1H, d, *J* = 3.0 Hz, ArH), 9.18 (1H, s, NH), 11.08 (1H, s, NH). <sup>13</sup>C NMR (100.6 MHz, CDCl<sub>3</sub>) δ = 67.40, 106.50, 109.83, 115.15, 115.49, 124.24, 130.73, 130.92, 133.17, 139.60, 139.70, 140.92, 149.06, 151.73, 161.52, 163.93, 167.06. HRMS (ES<sup>+</sup>): *m/z* calculated for C<sub>18</sub>H<sub>14</sub>F<sub>2</sub>N<sub>4</sub>O<sub>2</sub>: 357.1163 [M+H]<sup>+</sup>. Found 357.1176.

**1-(3-(3-Fluorobenzyloxy)pyrazin-2-yl)-3-(3,4-dichlorophenyl)urea (7dc)**

White solid, yield: 63.6%, mp: 162.8-163.7 °C, HPLC purity: 7.67 min, 94.31%, <sup>1</sup>H NMR (400 MHz, CDCl<sub>3</sub>) δ = 5.45 (2H, s, OCH<sub>2</sub>Ph), 7.06-7.08 (1H, m, ArH), 7.13-7.16 (1H, m, ArH), 7.22

(1H, d,  $J = 7.60$  Hz, ArH), 7.35-7.39 (2H, m, ArH), 7.43-7.46 (1H, m, ArH), 7.47 (1H, s, NH), 7.75 (1H, m, ArH), 7.77-7.78 (2H, m, ArH), 11.40 (1H, s, NH).  $^{13}\text{C}$  NMR (100.6 MHz,  $\text{CDCl}_3$ )  $\delta = 68.11, 107.61, 110.51, 115.51, 115.64$  ( $J_{\text{C-F}} = 23.2$  Hz), 124.08, 129.99, 130.37 ( $J_{\text{C-F}} = 8.2$  Hz), 131.65, 132.56, 137.75, 139.27, 139.57 ( $J_{\text{C-F}} = 11.0$  Hz), 147.80, 151.41, 162.98, 163.10 ( $J_{\text{C-F}} = 242.9$  Hz). HRMS ( $\text{ES}^+$ ):  $m/z$  calculated for  $\text{C}_{18}\text{H}_{13}\text{Cl}_2\text{FN}_4\text{O}_2$ : 407.0478  $[\text{M}+\text{H}]^+$ . Found 407.0496.

#### **1-(3-(3-Fluorobenzyloxy)pyrazin-2-yl)-3-(4-methylphenyl)urea (7dd)**

White solid, yield: 77.8%, mp: 173.0-173.5 °C, HPLC purity: 7.38 min, 100%,  $^1\text{H}$  NMR (400 MHz,  $\text{CDCl}_3$ )  $\delta = 2.32$  (3H, s,  $\text{CH}_3$ ), 5.44 (2H, s,  $\text{OCH}_2\text{Ph}$ ), 7.06-7.09 (1H, m, ArH), 7.15 (3H, d,  $J = 8.5$  Hz, ArH), 7.22 (1H, d,  $J = 7.7$  Hz, ArH), 7.34-7.38 (1H, m, ArH), 7.43 (1H, s, NH), 7.45 (2H, d,  $J = 8.4$  Hz, ArH), 7.70 (1H, d,  $J = 3.1$  Hz, ArH), 7.77 (1H, d,  $J = 3.1$  Hz, ArH), 11.15 (1H, s, NH).  $^{13}\text{C}$  NMR (100.6 MHz,  $\text{CDCl}_3$ )  $\delta = 19.83, 66.98, 114.45$  ( $J_{\text{C-F}} = 21.8$  Hz), 114.57 ( $J_{\text{C-F}} = 21.0$  Hz), 119.47, 123.02, 128.47, 129.27, 130.71, 131.13, 132.51, 134.24, 136.79, 138.48, 146.71, 150.59, 163.10 ( $J_{\text{C-F}} = 243.0$  Hz). HRMS ( $\text{ES}^+$ ):  $m/z$  calculated for  $\text{C}_{19}\text{H}_{17}\text{FN}_4\text{O}_2$ : 353.1414  $[\text{M}+\text{H}]^+$ . Found 353.1447.

#### **1-(3-(2-Chlorobenzyloxy)pyridin-2-yl)-3-phenylurea (7ea)**

White solid, yield: 93.3%, mp: 153.0-153.7 °C, HPLC purity: 7.26 min, 97.68%,  $^1\text{H}$  NMR (300 MHz,  $\text{DMSO-}d_6$ )  $\delta = 5.31$  (2H, s,  $\text{OCH}_2\text{Ph}$ ), 7.02-7.09 (2H, m, ArH), 7.32 (2H, t,  $J = 7.5$  Hz, ArH), 7.38-7.43 (2H, m, ArH), 7.53-7.90 (4H, m, ArH), 7.68-7.71 (1H, m, ArH), 7.96 (1H, d,  $J = 5.1$  Hz, ArH), 8.09 (1H, s, NH), 11.69 (1H, s, NH).  $^{13}\text{C}$  NMR (100.6 MHz,  $\text{CDCl}_3$ )  $\delta = 68.09, 116.90, 118.12, 120.28, 123.43, 127.33, 128.94, 129.49, 129.86, 130.04, 132.77, 133.36, 137.27,$

138.55, 141.28, 143.83, 152.31. HRMS (ES<sup>+</sup>): m/z calculated for C<sub>19</sub>H<sub>16</sub>ClN<sub>3</sub>O<sub>2</sub>: 354.1009 [M+H]<sup>+</sup>. Found 354.1072.

**1-(3-(2-Chlorobenzyloxy)pyridin-2-yl)-3-(2-fluorophenyl)urea (7eb)**

Yellow solid, yield: 78.1%, mp: 138.1-139.4 °C, HPLC purity: 7.44 min, 100%, <sup>1</sup>H NMR (400 MHz, DMSO-*d*<sub>6</sub>) δ = 5.32 (2H, s, OCH<sub>2</sub>Ph), 7.08 (2H, m, ArH), 7.18 (1H, t, *J* = 8.0 Hz, ArH), 7.26-7.31 (1H, dd, *J* = 1.2 Hz, 8.0 Hz, ArH), 7.41-7.43 (2H, m, ArH), 7.53-7.55 (1H, m, ArH), 7.57 (1H, d, *J* = 8.0 Hz, ArH), 7.69-7.71 (1H, m, ArH), 7.92 (1H, d, *J* = 8.0 Hz, ArH), 8.20-8.24 (1H, m, ArH), 8.31 (1H, s, NH), 12.01 (1H, s, NH). <sup>13</sup>C NMR (100.6 MHz, CDCl<sub>3</sub>) δ = 68.10, 114.74 (*J*<sub>C-F</sub> = 19.1 Hz), 117.10, 118.24, 121.72, 123.23 (*J*<sub>C-F</sub> = 7.3 Hz), 124.41, 127.20, 127.31, 129.49, 129.85, 130.04, 132.78, 133.37, 137.42, 141.20, 143.54, 152.16, 152.96 (*J*<sub>C-F</sub> = 242.4 Hz). HRMS (ES<sup>+</sup>): m/z calculated for C<sub>19</sub>H<sub>15</sub>ClFN<sub>3</sub>O<sub>2</sub>: 372.0915 [M+H]<sup>+</sup>. Found 372.0987.

**1-(3-(2-Chlorobenzyloxy)pyridin-2-yl)-3-(3-fluorophenyl)urea (7ec)**

White solid, yield: 76.0%, mp: 137.1-138.5 °C, HPLC purity: 7.35 min, 95.53%, <sup>1</sup>H NMR (400 MHz, CDCl<sub>3</sub>) δ = 5.24 (2H, s, OCH<sub>2</sub>Ph), 6.91-6.94 (1H, m, ArH), 7.18 (1H, d, *J* = 8.4 Hz, ArH), 7.30-7.54 (8H, m, ArH+NH), 7.80 (1H, s, ArH), 7.88 (1H, d, *J* = 4.8 Hz, ArH), 12.01 (1H, s, NH). <sup>13</sup>C NMR (100.6 MHz, CDCl<sub>3</sub>) δ = 68.16, 100.84, 107.43 (*J*<sub>C-F</sub> = 25.7 Hz), 109.95 (*J*<sub>C-F</sub> = 20.6 Hz), 115.41, 117.11, 118.27, 127.33, 129.52, 129.89, 130.10, 132.68, 133.40, 137.23, 140.16, 141.32, 143.66, 152.11, 163.24 (*J*<sub>C-F</sub> = 250.4 Hz). HRMS (ES<sup>+</sup>): m/z calculated for C<sub>19</sub>H<sub>15</sub>ClFN<sub>3</sub>O<sub>2</sub>: 372.0915 [M+H]<sup>+</sup>. Found 372.0982.

**1-(3-(2-Chlorobenzyloxy)pyridin-2-yl)-3-(3-chlorophenyl)urea (7ed)**

Yellow solid, yield: 61.9%, mp: 121.7-122.6 °C, HPLC purity: 7.58 min, 100%, <sup>1</sup>H NMR (400 MHz, DMSO-*d*<sub>6</sub>) δ = 5.31 (2H, OCH<sub>2</sub>Ph), 7.07-7.11 (2H, m, ArH), 7.34 (1H, t, *J* = 8.0 Hz, ArH), 7.40-7.43 (2H, m, ArH), 7.45-7.48 (1H, m, ArH), 7.53-7.57 (2H, m, ArH), 7.68-7.70 (1H, m, ArH), 7.82 (1H, t, *J* = 2.0 Hz, ArH), 7.98 (1H, dd, *J* = 1.2 Hz, 4.8 Hz, ArH), 8.24 (1H, s, NH), 11.82 (1H, s, NH). <sup>13</sup>C NMR (100.6 MHz, CDCl<sub>3</sub>) δ = 68.16, 117.15, 118.10, 118.30, 120.04, 123.61, 127.33, 129.51, 129.88, 130.09, 132.69, 133.39, 134.48, 137.21, 139.85, 141.31, 143.60, 152.09. HRMS (ES<sup>+</sup>): *m/z* calculated for C<sub>19</sub>H<sub>15</sub>Cl<sub>2</sub>N<sub>3</sub>O<sub>2</sub>: 388.0619 [M+H]<sup>+</sup>. Found 388.0652.

#### **1-(3-(2-Chlorobenzoyloxy)pyridin-2-yl)-3-(3,4-dichlorophenyl)urea (7ee)**

White solid, yield: 90.0%, mp: 135.0-135.7 °C, <sup>1</sup>H NMR (400 MHz, CDCl<sub>3</sub>) δ = 5.24 (2H, s, OCH<sub>2</sub>Ph), 6.74-6.78 (1H, m, ArH), 6.91 (1H, dd, *J* = 5.2 Hz, 8.0 Hz, ArH), 7.17 (1H, d, *J* = 7.6 Hz, ArH), 7.25-7.27 (1H, m, ArH), 7.30-7.35 (2H, m, ArH), 7.43-7.46 (2H, m, ArH), 7.52-7.55 (2H, m, ArH+NH), 7.88 (1H, d, *J* = 8.0 Hz, ArH), 11.98 (1H, s, NH). <sup>13</sup>C NMR (100.6 MHz, CDCl<sub>3</sub>) δ = 68.21, 117.30, 118.42, 119.32, 121.55, 126.27, 127.32, 129.52, 129.89, 130.12, 130.35, 132.54, 132.64, 133.42, 137.18, 138.22, 141.34, 143.45, 152.03. HRMS (ES<sup>+</sup>): *m/z* calculated for C<sub>19</sub>H<sub>14</sub>Cl<sub>3</sub>N<sub>3</sub>O<sub>2</sub>: 422.0230 [M+H]<sup>+</sup>. Found 422.0236.

#### **1-(3-(2-Chlorobenzoyloxy)pyridin-2-yl)-3-(4-methylphenyl)urea (7ef)**

White solid, yield: 89.8%, mp: 151.6-152.8 °C, HPLC purity: 7.47 min, 97.54%, <sup>1</sup>H NMR (400 MHz, CDCl<sub>3</sub>) δ = 2.32 (3H, s, CH<sub>3</sub>), 5.23 (2H, s, OCH<sub>2</sub>Ph), 6.89 (1H, dd, *J* = 5.2 Hz, 8.0 Hz, ArH), 7.13-7.15 (3H, m, ArH), 7.31-7.34 (2H, m, ArH), 7.43-7.47 (2H, m, ArH), 7.48 (2H, d, *J* = 8.4 Hz, ArH), 7.50 (1H, s, NH), 7.87 (1H, dd, *J* = 1.2 Hz, 5.2 Hz, ArH), 11.71 (1H, s, NH). <sup>13</sup>C NMR (100.6 MHz, CDCl<sub>3</sub>) δ = 20.86, 68.05, 116.76, 118.02, 120.40, 127.32, 129.44, 129.84,

130.01, 132.80, 132.96, 133.33, 135.89, 137.28, 141.25, 143.91, 152.36. HRMS (ES<sup>+</sup>): m/z calculated for C<sub>20</sub>H<sub>18</sub>ClN<sub>3</sub>O<sub>2</sub>: 368.1166 [M+H]<sup>+</sup>. Found 368.1189.

**1-(3-(2-Chlorobenzyloxy)pyridin-2-yl)-3-(naphthalen-1-yl)urea (7eg)**

Yellow solid, yield: 90.1%, mp: 224.1-226.4 °C, HPLC purity: 7.67 min, 95.86%, <sup>1</sup>H NMR (400 MHz, DMSO-*d*<sub>6</sub>) δ = 5.36 (2H, s, OCH<sub>2</sub>Ph), 7.15 (1H, dd, *J* = 5.2 Hz, 8.0 Hz, ArH), 7.42-7.44 (2H, m, ArH), 7.49-7.60 (3H, m, ArH), 7.62 (1H, dd, *J* = 1.2 Hz, 8.0 Hz, ArH), 7.66-7.74 (3H, m, ArH), 7.98 (1H, d, *J* = 8.0 Hz, ArH), 8.11 (1H, dd, *J* = 1.2 Hz, 8.0 Hz, ArH), 8.27 (1H, s, NH), 8.16-8.21 (2H, m, ArH), 12.38 (1H, s, NH). <sup>13</sup>C NMR (100.6 MHz, DMSO-*d*<sub>6</sub>) δ = 68.49, 117.63, 118.29, 120.71, 121.26, 123.95, 125.99, 126.43, 126.53, 127.03, 127.94, 129.12, 129.98, 130.74, 131.09, 133.24, 133.80, 134.19, 134.31, 137.75, 141.96, 143.96, 152.31. HRMS (ES<sup>+</sup>): m/z calculated for C<sub>23</sub>H<sub>18</sub>ClN<sub>3</sub>O<sub>2</sub>: 404.1166 [M+H]<sup>+</sup>. Found 404.1191.

**1-(3-(3-Chlorobenzyloxy)pyridin-2-yl)-3-phenylurea (7fa)**

White solid, yield: 99.0%, mp: 102.5-103.9 °C, HPLC purity: 7.19 min, 100%, <sup>1</sup>H NMR (400 MHz, DMSO-*d*<sub>6</sub>) δ = 5.27 (2H, s, OCH<sub>2</sub>Ph), 7.02-7.05 (2H, m, ArH), 7.33 (2H, t, *J* = 7.6 Hz, ArH), 7.41-7.44 (2H, m, ArH), 7.48-7.51 (2H, m, ArH), 7.58 (2H, d, *J* = 8.0 Hz, ArH), 7.69 (1H, s, ArH), 7.94 (1H, d, *J* = 4.8 Hz, ArH), 8.37 (1H, s, NH), 11.72 (1H, s, NH). <sup>13</sup>C NMR (100.6 MHz, CDCl<sub>3</sub>) δ = 69.98, 116.86, 117.99, 120.22, 123.42, 125.80, 127.80, 128.94, 130.28, 134.81, 137.13, 137.24, 138.57, 141.21, 143.74, 152.25. HRMS (ES<sup>+</sup>): m/z calculated for C<sub>19</sub>H<sub>16</sub>ClN<sub>3</sub>O<sub>2</sub>: 354.1009 [M+H]<sup>+</sup>. Found 354.1096.

**1-(3-(3-Chlorobenzyloxy)pyridin-2-yl)-3-(2-fluorophenyl)urea (7fb)**

White solid, yield: 80.5%, mp: 118.9-119.4 °C, HPLC purity: 7.38 min, 100%, <sup>1</sup>H NMR (400 MHz, DMSO-*d*<sub>6</sub>) δ = 5.27 (2H, s, OCH<sub>2</sub>Ph), 7.03-7.10 (2H, m, ArH), 7.18 (1H, t, *J* = 7.6 Hz, ArH), 7.26-7.31 (1H, m, ArH), 7.39-7.45 (2H, m, ArH), 7.50-7.53 (2H, m, ArH), 7.70 (1H, s, ArH), 7.78 (1H, d, *J* = 5.2 Hz, ArH), 8.24 (1H, td, *J* = 1.4 Hz, 8.1 Hz, ArH), 8.65 (1H, s, NH), 12.06 (1H, s, NH). <sup>13</sup>C NMR (100.6 MHz, CDCl<sub>3</sub>) δ = 70.03, 114.75 (*J*<sub>C-F</sub> = 18.9 Hz), 117.02, 118.05, 121.73, 123.26 (*J*<sub>C-F</sub> = 7.3 Hz), 124.45, 125.78, 127.21 (*J*<sub>C-F</sub> = 10.2 Hz), 127.82, 128.97, 130.29, 134.85, 137.07, 137.42, 141.15, 152.11, 152.96 (*J*<sub>C-F</sub> = 242.5 Hz). HRMS (ES<sup>+</sup>): *m/z* calculated for C<sub>19</sub>H<sub>15</sub>ClFN<sub>3</sub>O<sub>2</sub>: 372.0915 [M+H]<sup>+</sup>. Found 372.0985.

#### **1-(3-(3-Chlorobenzyloxy)pyridin-2-yl)-3-(3-fluorophenyl)urea (7fc)**

White solid, yield: 61.2%, mp: 114.0-114.7 °C, HPLC purity: 7.30 min, 96.43%, <sup>1</sup>H NMR (400 MHz, DMSO-*d*<sub>6</sub>) δ = 5.26 (2H, s, OCH<sub>2</sub>Ph), 6.84-6.89 (1H, m, ArH), 7.06 (1H, dd, *J* = 5.2 Hz, 8.0 Hz, ArH), 7.29-7.32 (1H, m, ArH), 7.35 (1H, d, *J* = 6.8 Hz, ArH), 7.38-7.45 (2H, m, ArH), 7.49-7.52 (2H, m, ArH), 7.60-7.64 (1H, dt, *J* = 2.4 Hz, 12.0 Hz, ArH), 7.69 (1H, s, ArH), 7.95 (1H, dd, *J* = 1.2 Hz, 5.2 Hz, ArH), 8.54 (1H, s, NH), 11.87 (1H, s, NH). <sup>13</sup>C NMR (100.6 MHz, CDCl<sub>3</sub>) δ = 70.03, 107.37 (*J*<sub>C-F</sub> = 26.0 Hz), 109.82 (*J*<sub>C-F</sub> = 21.2 Hz), 115.37, 117.09, 118.14, 125.78, 127.79, 128.95, 129.89 (*J*<sub>C-F</sub> = 9.3 Hz), 130.29, 134.83, 137.04, 137.19, 140.22 (*J*<sub>C-F</sub> = 10.9 Hz), 141.25, 143.53, 152.08, 163.13 (*J*<sub>C-F</sub> = 242.2 Hz). HRMS (ES<sup>+</sup>): *m/z* calculated for C<sub>19</sub>H<sub>15</sub>ClFN<sub>3</sub>O<sub>2</sub>: 372.0915 [M+H]<sup>+</sup>. Found 372.0990.

#### **1-(3-(3-Chlorobenzyloxy)pyridin-2-yl)-3-(3-chlorophenyl)urea (7fd)**

White solid, yield: 90.0%, mp: 103.2-104.7 °C, HPLC purity: 7.51 min, 100%, <sup>1</sup>H NMR (400 MHz, DMSO-*d*<sub>6</sub>) δ = 5.26 (2H, OCH<sub>2</sub>Ph), 7.06 (1H, dd, *J* = 5.2 Hz, 8.0 Hz, ArH), 7.10 (1H, dd,

$J = 2.0$  Hz,  $8.0$  Hz, ArH),  $7.34$  (1H, t,  $J = 8.0$  Hz, ArH),  $7.41$ - $7.52$  (5H, m, ArH),  $7.69$  (1H, s, ArH),  $7.83$  (1H, t,  $J = 2.0$  Hz, ArH),  $7.95$  (1H, d,  $J = 5.2$  Hz, ArH),  $8.56$  (1H, s, NH),  $11.86$  (1H, s, NH).  $^{13}\text{C}$  NMR (100.6 MHz, DMSO- $d_6$ )  $\delta = 74.21, 122.98, 123.07, 123.93, 125.06, 127.71, 131.69, 132.97, 133.27, 135.52, 135.66, 138.43, 138.51, 142.39, 143.83, 145.51, 146.89, 148.30, 156.85$ . HRMS (ES $^+$ ):  $m/z$  calculated for  $\text{C}_{19}\text{H}_{15}\text{Cl}_2\text{N}_3\text{O}_2$ :  $388.0619$  [M+H] $^+$ . Found  $388.0644$ .

**1-(3-(3-Chlorobenzyloxy)pyridin-2-yl)-3-(3,4-dichlorophenyl)urea (7fe)**

White solid, yield: 89.7%, mp:  $122.8$ - $123.5$  °C, HPLC purity:  $7.74$  min, 100%,  $^1\text{H}$  NMR (400 MHz,  $\text{CDCl}_3$ )  $\delta = 5.11$  (2H, s,  $\text{OCH}_2\text{Ph}$ ),  $6.91$  (1H, dd,  $J = 5.2$  Hz,  $8.0$  Hz, ArH),  $7.13$  (1H, dd,  $J = 1.2$  Hz,  $8.0$  Hz, ArH),  $7.29$ - $7.30$  (1H, m, ArH),  $7.36$ - $7.38$  (4H, m, ArH),  $7.48$  (1H, dd,  $J = 2.4$  Hz,  $8.8$  Hz, ArH),  $7.51$  (1H, s, NH),  $7.80$  (1H, d,  $J = 2.4$  Hz, ArH),  $7.88$  (1H, dd,  $J = 1.2$  Hz,  $5.2$  Hz, ArH),  $12.01$  (1H, s, NH).  $^{13}\text{C}$  NMR (100.6 MHz,  $\text{CDCl}_3$ )  $\delta = 70.10, 117.20, 118.21, 119.35, 121.57, 125.77, 126.31, 127.82, 129.04, 130.32, 130.37, 132.56, 134.90, 136.93, 137.20, 138.19, 141.28, 143.44, 151.98$ . HRMS (ES $^+$ ):  $m/z$  calculated for  $\text{C}_{19}\text{H}_{14}\text{Cl}_3\text{N}_3\text{O}_2$ :  $422.0230$  [M+H] $^+$ . Found  $422.0248$ .

**1-(3-(3-Chlorobenzyloxy)pyridin-2-yl)-3-(4-methylphenyl)urea (7ff)**

White solid, yield: 89.8%, mp:  $128.0$ - $128.4$  °C, HPLC purity:  $7.37$  min, 97.48%,  $^1\text{H}$  NMR (400 MHz,  $\text{CDCl}_3$ )  $\delta = 2.32$  (3H, s,  $\text{CH}_3$ ),  $5.09$  (2H, s,  $\text{OCH}_2\text{Ph}$ ),  $6.87$  (1H, dd,  $J = 4.8$  Hz,  $8.0$  Hz, ArH),  $7.09$  (1H, dd,  $J = 1.2$  Hz,  $8.0$  Hz, ArH),  $7.14$  (2H, d,  $J = 8.4$  Hz, ArH),  $7.25$ - $7.30$  (1H, m, ArH),  $7.35$ - $7.36$  (2H, m, ArH),  $7.38$  (1H, s, NH),  $7.47$  (2H, s, ArH),  $7.49$  (1H, s, ArH),  $7.86$  (1H, dd,  $J = 1.2$  Hz,  $4.8$  Hz, ArH),  $11.71$  (1H, s, NH).  $^{13}\text{C}$  NMR (100.6 MHz,  $\text{CDCl}_3$ )  $\delta = 20.87, 69.98, 116.73, 117.90, 120.37, 125.78, 127.79, 128.92, 129.45, 130.28, 132.98, 134.82, 135.88, 137.13,$

137.26, 141.19, 143.82, 152.33. HRMS (ES<sup>+</sup>): m/z calculated for C<sub>20</sub>H<sub>18</sub>ClN<sub>3</sub>O<sub>2</sub>: 368.1166 [M+H]<sup>+</sup>. Found 368.1182.

**1-(3-(3-Chlorobenzyloxy)pyridin-2-yl)-3-(4-trifluoromethylphenyl)urea (7fg)**

White solid, 60.0%, mp: 142.6-142.9 °C, HPLC purity: 7.38 min, 100%, <sup>1</sup>H NMR (400 MHz, CDCl<sub>3</sub>) δ = 5.11 (2H, s, OCH<sub>2</sub>Ph), 6.92 (1H, dd, *J* = 5.2 Hz, 8.0 Hz, ArH), 7.13 (1H, dd, *J* = 1.2 Hz, 8.0 Hz, ArH), 7.28-7.31 (1H, m, ArH), 7.36-7.39 (3H, m, ArH), 7.54 (1H, s, NH), 7.58 (2H, d, *J* = 8.4 Hz, ArH), 7.73 (2H, d, *J* = 8.4 Hz, ArH), 8.89 (1H, dd, *J* = 1.2, 5.2 Hz, ArH), 11.71 (1H, s, NH). <sup>13</sup>C NMR (100.6 MHz, CDCl<sub>3</sub>) δ = 69.54, 115.35, 118.29, 120.28, 121.51, 123.75, 125.07, 127.38, 128.92, 130.33, 133.27, 135.50, 137.19, 141.94, 143.59, 151.45, 151.92, 153.86.

**1-(3-(3-Chlorobenzyloxy)pyridin-2-yl)-3-(naphthalen-1-yl)urea (7fh)**

White solid, yield: 90.1%, mp: 206.5-207.9 °C, HPLC purity: 7.61 min, 95.49%, <sup>1</sup>H NMR (300 MHz, DMSO-*d*<sub>6</sub>) δ = 5.31 (2H, s, OCH<sub>2</sub>Ph), 7.11 (1H, dd, *J* = 8.1 Hz, 5.1 Hz, ArH), 7.43-7.45 (2H, m, ArH), 7.48-7.60 (4H, m, ArH), 7.66-7.73 (3H, m, ArH), 7.97 (1H, d, *J* = 7.2 Hz, ArH), 8.08 (1H, d, *J* = 5.4 Hz, ArH), 8.17 (1H, d, *J* = 8.4 Hz, ArH), 8.22 (1H, d, *J* = 7.8 Hz, ArH), 8.63 (1H, s, NH), 12.45 (1H, s, NH). <sup>13</sup>C NMR (100.6 MHz, DMSO-*d*<sub>6</sub>) δ = 69.51, 117.56, 117.88, 118.11, 120.31, 121.26, 123.84, 125.96, 126.43, 126.98, 128.28, 128.56, 129.11, 130.80, 133.69, 134.19, 134.41, 137.37, 139.06, 141.95, 144.01, 152.48. HRMS (ES<sup>+</sup>): m/z calculated for C<sub>23</sub>H<sub>18</sub>ClN<sub>3</sub>O<sub>2</sub>: 404.1166 [M+H]<sup>+</sup>. Found 404.1188.

**1-(3-(4-Chlorobenzyloxy)pyridin-2-yl)-3-(2-fluorophenyl)urea (7ga)**

White solid, yield: 63.1%, mp: 134.8-135.2 °C, HPLC purity: 7.47 min, 100%, <sup>1</sup>H NMR (400 MHz, DMSO-*d*<sub>6</sub>) δ = 5.32 (2H, s, OCH<sub>2</sub>Ph), 7.08 (2H, m, ArH), 7.18 (1H, t, *J* = 8.0 Hz, ArH), 7.26-7.31 (1H, dd, *J* = 1.2 Hz, 8.0 Hz, ArH), 7.41-7.43 (2H, m, ArH), 7.53-7.55 (1H, m, ArH), 7.57 (1H, d, *J* = 8.0 Hz, ArH), 7.69-7.71 (1H, m, ArH), 7.92 (1H, d, *J* = 8.0 Hz, ArH), 8.20-8.24 (1H, m, ArH), 8.31 (1H, s, NH), 12.01 (1H, s, NH). <sup>13</sup>C NMR (100.6 MHz, CDCl<sub>3</sub>) δ = 69.54, 118.42, 119.53, 120.36, 123.13, 123.45, 126.27, 126.59, 128.90, 130.29, 133.25, 135.51, 137.55, 142.20, 142.92, 143.44, 152.01.

**1-(3-(4-Chlorobenzoyloxy)pyridin-2-yl)-3-(3-fluorophenyl)urea (7gb)**

White solid, yield: 43.3%, mp: 117.8-118.8 °C, HPLC purity: 7.33 min, 94.37%, <sup>1</sup>H NMR (400 MHz, CDCl<sub>3</sub>) δ = 5.11 (2H, s, OCH<sub>2</sub>Ph), 6.74-6.79 (1H, m, ArH), 6.88-6.91 (1H, m, ArH), 7.12 (1H, dd, *J* = 1.3 Hz, 8.0 Hz, ArH), 7.26-7.29 (2H, m, ArH), 7.33-7.41 (4H, m, ArH), 7.49 (1H, s, NH), 7.52-7.55 (1H, m, ArH), 7.86 (1H, dd, *J* = 1.3 Hz, 5.1, ArH), 11.97 (1H, s, NH). HRMS (ES<sup>+</sup>): *m/z* calculated for C<sub>19</sub>H<sub>15</sub>ClFN<sub>3</sub>O<sub>2</sub>: 394.0735 [M+Na]<sup>+</sup>. Found 394.0737.

**1-(3-(4-Chlorobenzoyloxy)pyridin-2-yl)-3-(3-chlorophenyl)urea (7gc)**

Yellow solid, yield: 12.0%, mp: 138.0-139.9 °C, <sup>1</sup>H NMR (400 MHz, CDCl<sub>3</sub>) δ = 5.10 (2H, s, OCH<sub>2</sub>Ph), 6.90 (1H, dd, *J* = 8.0 Hz, 5.2 Hz, ArH), 7.03-7.06 (1H, m, ArH), 7.12 (1H, dd, *J* = 1.2 Hz, 8.0 Hz, ArH), 7.24 (1H, t, *J* = 8.4 Hz, ArH), 7.34 (2H, d, *J* = 8.4 Hz, ArH), 7.40 (2H, d, *J* = 8.4 Hz, ArH), 7.48-7.50 (2H, m, ArH+NH), 7.68 (1H, t, *J* = 2.4 Hz, ArH), 7.87 (1H, dd, *J* = 1.2 Hz, 5.2 Hz, ArH), 11.95 (1H, s, NH). HRMS (ES<sup>+</sup>): *m/z* calculated for C<sub>19</sub>H<sub>15</sub>Cl<sub>2</sub>N<sub>3</sub>O<sub>2</sub>: 410.0439 [M+Na]<sup>+</sup>. Found 410.0436.

**1-(3-(4-Chlorobenzoyloxy)pyridin-2-yl)-3-(3,4-dichlorophenyl)urea (7gd)**

White solid, yield: 66.1%, mp: 161.9-162.5 °C, <sup>1</sup>H NMR (400 MHz, CDCl<sub>3</sub>) δ = 5.11 (2H, s, OCH<sub>2</sub>Ph), 6.89-6.92 (1H, m, ArH), 7.13 (1H, dd, *J* = 5.2 Hz, 8.0 Hz, ArH), 7.33-7.41 (5H, m, ArH), 7.47 (1H, dd, *J* = 2.5 Hz, 8.7 Hz, ArH), 7.51 (1H, s, NH), 7.80 (1H, d, *J* = 2.5 Hz, ArH), 7.87 (1H, dd, *J* = 1.2 Hz, 5.0 Hz, ArH), 12.00 (1H, s, NH). <sup>13</sup>C NMR (100.6 MHz, DMSO-*d*<sub>6</sub>) δ = 69.54, 117.93, 118.66, 119.83, 120.08, 128.95, 129.61, 129.75, 130.34, 132.28, 133.26, 135.56, 136.57, 137.47, 141.83, 143.79, 151.97. HRMS (ES<sup>+</sup>): *m/z* calculated for C<sub>19</sub>H<sub>14</sub>Cl<sub>3</sub>N<sub>3</sub>O<sub>2</sub>: 444.0050 [M+Na]<sup>+</sup>. Found 444.0034.

**1-(3-(4-Chlorobenzoyloxy)pyridin-2-yl)-3-(4-methylphenyl)urea (7ge)**

Yellow solid, yield: 90.4%, mp: 111.7-114.3 °C, HPLC purity: 7.40 min, 90.54%, <sup>1</sup>H NMR (300 MHz, DMSO-*d*<sub>6</sub>) δ = 2.26 (3H, s, CH<sub>3</sub>), 5.25 (2H, s, OCH<sub>2</sub>Ph), 7.02 (1H, dd, *J* = 5.1 Hz, 8.1 Hz, ArH), 7.13 (2H, d, *J* = 8.1 Hz, ArH), 7.44-7.49 (5H, m, ArH), 7.58 (2H, d, *J* = 8.4 Hz, ArH), 7.91 (1H, d, *J* = 5.1 Hz, ArH), 8.18 (1H, s, NH), 11.64 (1H, s, NH). <sup>13</sup>C NMR (100.6 MHz, CDCl<sub>3</sub>) δ = 20.85, 69.54, 117.93, 118.66, 119.83, 128.95, 129.61, 130.34, 132.28, 133.26, 135.56, 136.57, 137.47, 141.83, 143.79, 151.97. HRMS (ES<sup>+</sup>): *m/z* calculated for C<sub>20</sub>H<sub>18</sub>ClN<sub>3</sub>O<sub>2</sub>: 368.1166 [M+H]<sup>+</sup>. Found 368.1171.

**1-(3-(4-Chlorobenzoyloxy)pyridin-2-yl)-3-(4-trifluoromethylphenyl)urea (7gf)**

White solid, yield: 24.1%, mp: 127.6-128.3 °C, HPLC purity: 7.47 min, 100%, <sup>1</sup>H NMR (400 MHz, CDCl<sub>3</sub>) δ = 5.11 (2H, s, OCH<sub>2</sub>Ph), 6.90 (1H, dd, *J* = 5.2 Hz, 8.0 Hz, ArH), 7.13 (1H, dd, *J* = 0.8 Hz, 8.0 Hz, ArH), 7.34 (2H, d, *J* = 8.4 Hz, ArH), 7.40 (2H, d, *J* = 8.4 Hz, ArH), 7.52 (1H, s, NH), 7.58 (2H, d, *J* = 8.4 Hz, ArH), 7.73 (2H, d, *J* = 8.4 Hz, ArH), 7.88 (1H, *J* = 1.2 Hz, 5.2 Hz,

ArH), 12.12 (1H, s, NH).  $^{13}\text{C}$  NMR (100.6 MHz,  $\text{CDCl}_3$ )  $\delta$  = 69.45, 118.40, 119.51, 120.30, 126.51, 126.55, 128.18, 128.48, 130.70, 133.68, 137.57, 139.02, 142.22, 142.93, 143.46, 150.07. HRMS ( $\text{ES}^+$ ):  $m/z$  calculated for  $\text{C}_{20}\text{H}_{15}\text{ClF}_3\text{N}_3\text{O}_2$ : 422.0883  $[\text{M}+\text{H}]^+$ . Found 422.0885.

**1-(3-(4-Chlorobenzyloxy)pyridin-2-yl)-3-(naphthalen-1-yl)urea (7gg)**

White solid, yield: 97.8%, mp: 161.8-169.8 °C,  $^1\text{H}$  NMR (400 MHz,  $\text{CDCl}_3$ )  $\delta$  = 5.14 (2H, s,  $\text{OCH}_2\text{Ph}$ ), 6.93 (1H, dd,  $J$  = 5.2 Hz, 8.0 Hz, ArH), 7.16 (1H, d,  $J$  = 8.0 Hz, ArH), 7.37 (2H, d,  $J$  = 8.4 Hz, ArH), 7.41 (2H, d,  $J$  = 8.4 Hz, ArH), 7.49-7.57 (3H, m, ArH), 7.63 (1H, brs, ArH), 7.65 (1H, s, NH), 7.87 (1H, d,  $J$  = 8.0 Hz, ArH), 7.98 (1H, d,  $J$  = 5.2 Hz, ArH), 8.22 (2H, d,  $J$  = 7.6 Hz, ArH), 12.39 (1H, s, NH).  $^{13}\text{C}$  NMR (100.6 MHz,  $\text{DMSO}-d_6$ )  $\delta$  = 69.61, 117.56, 118.10, 120.34, 121.25, 121.93, 123.36, 123.86, 126.42, 126.49, 126.99, 128.95, 130.36, 133.29, 134.19, 134.38, 135.51, 137.32, 141.91, 143.96, 152.41. HRMS ( $\text{ES}^+$ ):  $m/z$  calculated for  $\text{C}_{23}\text{H}_{18}\text{ClN}_3\text{O}_2$ : 404.1166  $[\text{M}+\text{H}]^+$ . Found 404.1183.

**1-(3-(4-Fluorobenzyloxy)pyridin-2-yl)-3-(2-fluorophenyl)urea (7ha)**

White solid, yield: 62.3%, mp: 115.0-115.5 °C, HPLC purity: 7.17 min, 98.79%,  $^1\text{H}$  NMR (400 MHz,  $\text{CDCl}_3$ )  $\delta$  = 5.09 (2H, s,  $\text{OCH}_2\text{Ph}$ ), 6.90 (1H, dd,  $J$  = 4.8 Hz, 8.0 Hz, ArH), 7.00-7.03 (1H, m, ArH), 7.07-7.16 (5H, m, ArH), 7.37-7.41 (2H, m, ArH), 7.52 (1H, s, NH), 7.90 (1H, dd,  $J$  = 1.2 Hz, 4.8 Hz, ArH), 8.30-8.34 (1H, m, ArH), 12.20 (1H, s, NH).  $^{13}\text{C}$  NMR (100.6 MHz,  $\text{CDCl}_3$ )  $\delta$  = 69.69, 115.31, 115.84, 118.26, 120.24, 121.51, 123.66, 125.06, 127.36, 130.74, 132.65, 137.12, 141.97, 143.58, 151.60, 153.86, 162.20. HRMS ( $\text{ES}^+$ ):  $m/z$  calculated for  $\text{C}_{19}\text{H}_{15}\text{F}_2\text{N}_3\text{O}_2$ : 356.1210  $[\text{M}+\text{H}]^+$ . Found 356.1230.

**1-(3-(4-Fluorobenzyloxy)pyridin-2-yl)-3-(3-fluorophenyl)urea (7hb)**

White solid, yield: 92.3%, mp: 135.4-136.6 °C, HPLC purity: 7.08 min, 99.11%, <sup>1</sup>H NMR (400 MHz, CDCl<sub>3</sub>) δ = 5.09 (2H, s, OCH<sub>2</sub>Ph), 6.74-6.78 (1H, m, ArH), 6.89 (1H, dd, *J* = 5.2 Hz, 8.0 Hz, ArH), 7.09-7.16 (3H, m, ArH), 7.25-7.27 (2H, m, ArH), 7.37-7.40 (2H, m, ArH), 7.49 (1H, s, NH), 7.51-7.55 (1H, m, ArH), 7.86 (1H, *J* = 1.6 Hz, 5.2 Hz, ArH), 11.98 (1H, s, NH). <sup>13</sup>C NMR (100.6 MHz, CDCl<sub>3</sub>) δ = 70.22, 107.40 (*J*<sub>C-F</sub> = 21.2 Hz), 109.95 (*J*<sub>C-F</sub> = 21.1 Hz), 115.38, 115.85, 116.06, 117.05, 118.09, 129.82, 129.91, 130.81, 137.07, 140.23 (*J*<sub>C-F</sub> = 11.1 Hz), 141.40, 143.62, 152.10, 162.96 (*J*<sub>C-F</sub> = 247.5 Hz). HRMS (ES<sup>+</sup>): *m/z* calculated for C<sub>19</sub>H<sub>15</sub>F<sub>2</sub>N<sub>3</sub>O<sub>2</sub>: 356.1210 [M+H]<sup>+</sup>. Found 356.1235.

**1-(3-(4-Fluorobenzyloxy)pyridin-2-yl)-3-(3-chlorophenyl)urea (7hc)**

White solid, yield: 84.2%, mp: 90.9-94.1 °C, HPLC purity: 7.31 min, 91.98%, <sup>1</sup>H NMR (400 MHz, CDCl<sub>3</sub>) δ = 5.09 (2H, s, OCH<sub>2</sub>Ph), 6.90 (1H, dd, *J* = 4.8 Hz, 8.0 Hz, ArH), 7.04 (1H, d, *J* = 8.0 Hz, ArH), 7.09-7.16 (3H, m, ArH), 7.22-7.26 (1H, m, ArH), 7.37-7.40 (2H, m, ArH), 7.48-7.50 (2H, m, ArH), 7.67 (1H, s, NH), 7.87 (1H, d, *J* = 4.8 Hz, ArH), 11.96 (1H, s, NH). <sup>13</sup>C NMR (100.6 MHz, DMSO-*d*<sub>6</sub>) δ = 69.68, 115.76 (*J*<sub>C-F</sub> = 22.1 Hz), 117.29, 118.23, 119.17, 120.33, 122.99, 130.85, 132.75, 133.76, 137.50, 140.37, 141.47, 142.12, 143.51, 152.02, 162.44 (*J*<sub>C-F</sub> = 244.5 Hz). HRMS (ES<sup>+</sup>): *m/z* calculated for C<sub>19</sub>H<sub>15</sub>ClFN<sub>3</sub>O<sub>2</sub>: 372.0915 [M+H]<sup>+</sup>. Found 372.0990.

**4.2. Biological evaluation****4.2.1. Cell culture**

HT-22 (mouse hippocampal cells) cells were grown in Dulbecco's Modified Eagle's Medium (DMEM, GIBCO) supplemented with 10% (v/v) FBS and antibiotics (100 µg/mL penicillin/streptomycin mix) in a humidified atmosphere at 37 °C with 5% CO<sub>2</sub>.

#### **4.2.2. Protection against loss of mitochondrial membrane potential assay**

HT-22 cells (30,000 per well) were seeded into a clear 96-well plate (FALCON) at 200 µL per well one day prior to assay. 750 µM of JC-1 (Stratagene) in DMSO stock solution was dissolved into phenol red-free Opti-MEM (GIBCO) medium to make final concentration of 7.5 µM JC-1 per well. Medium was removed from the plate, and 100 µL per well of JC-1 was added. Plates were incubated for 1 h and 15 min at 37 °C and washed twice with 100 µL per well PBS. Subsequently, cells were treated with 25 µL solution of each compound at 5 µM in Opti-MEM and incubated at 37 °C for 10 min followed by addition of 25 µL of Aβ (American peptide, 1–42) solution at 5 µM. Fluorescence was measured at every 1 h for 3 h at ex/em 530 nm/580 nm ('red') and ex/em 485 nm/530 nm ('green'). The ratio of green to red fluorescence was recorded and the percent changes in ratio from each compound were calculated and normalized using vehicle control as 100%.

#### **4.2.3. Assay for cellular ATP levels (Luciferase-based assay)**

10,000 HT-22 cells per well were seeded into a clear 96-well plate (FALCON) at 200 µL per well one day prior to assay. Medium was removed from the plate, and cells were treated with 25 µL solution of each compound at 10 µM and incubated at 37 °C for 10 min followed by addition of 25 µL of amyloid Beta (American peptide, 1–42) solution at 10 µM. Cells were incubated at 37 °C for 7 h and washed twice with PBS. Cells were lysed by using 1% Triton-X 100 in TBST

buffer solution and protein concentrations of each well were determined via BCA protein determination kit (Thermo scientific). Equal amount of cell lysates from each well were plated into a white 96-well plate (NUNC) and the amount of ATP levels in each sample was determined by using ATP determination kit (Invitrogen). The ATP levels of each sample were subtracted with vehicle control and percent recovery were calculated based on the ATP levels of the vehicle control treated with amyloid Beta. Assessment of compounds' effect on ATP production was based on the ATP levels of each compound treated sample without the treatment with amyloid Beta solution.

#### **4.2.4. Cell viability MTT assay**

5000 HT-22 cells per well were seeded and treated as above described method. Cells were incubated at 37 °C for 24 h. 10 µL of MTT solution (Thiazolyl blue tetrazolium bromide, Sigma) was added directly to each well and incubated at 37 °C for 2 h. After confirming the formation of blue formazan precipitates under microscope, 140 µL of solubilizing solution (10% Triton-X 100 in isopropanol with 0.1 M HCl) was added to each well followed by incubation for another hour at room temperature. Absorbance at 570 nM was measured and OD values from each well were subtracted with vehicle control and percent compounds' direct effect on viability and protective effect against amyloid Beta induced cytotoxicity were calculated by using the same method described for the ATP assay.

#### **4.2.5. Molecular docking**

The three-dimensional structure of human CypD in complex with CsA (pdb code: 2Z6W) was retrieved from protein databank. Using protein preparation tool in Discovery Studio 4.0

(Accelrys, San Diego, CA, USA), the receptor was prepared for docking. Ligands were sketched in ChemBioDraw program and then prepared generating the minimized 3D structures using Ligand Preparation tool in Discovery Studio 4.0. Docking minimization were done using CDocker algorithm implemented in Discovery Studio 4.0. The calculated docked poses were subjected to *in situ* ligand minimization within the binding pocket with estimation of binding energy and complex energy. The results were visualized and analyzed using tools implemented in Discovery Studio 4.0.

### Acknowledgments

This work was supported by the KIST Institutional programs (Grant No. 2E27000) from Korea Institute of Science and Technology and by the Creative Fusion Research Program through the Creative Allied Project funded by the National Research Council of Science & Technology (CAP-12-1-KIST).

### References

- [1] P. Bernardi, K. Broekemeier, D. Pfeiffer, Recent progress on regulation of the mitochondrial permeability transition pore; a cyclosporin-sensitive pore in the inner mitochondrial membrane, *J Bioenerg Biomembr*, 26 (1994) 509-517.
- [2] M.R. Duchon, Roles of Mitochondria in Health and Disease, *Diabetes*, 53 (2004) S96-S102.
- [3] E. Yehuda-Shnaidman, B. Kalderon, N. Azazmeh, J. Bar-Tana, Gating of the mitochondrial permeability transition pore by thyroid hormone, *The FASEB Journal*, 24 (2010) 93-104.
- [4] P. Bernardi, The mitochondrial permeability transition pore: a mystery solved?, *Frontiers in physiology*, 4 (2013) 95.
- [5] P. Bernardi, P. Bonaldo, Mitochondrial Dysfunction and Defective Autophagy in the Pathogenesis of Collagen VI Muscular Dystrophies, *Cold Spring Harbor Perspectives in Biology*, 5 (2013).
- [6] A. Rasola, P. Bernardi, The mitochondrial permeability transition pore and its adaptive responses in tumor cells, *Cell Calcium*, 56 (2014) 437-445.
- [7] P. Bernardi, F. Di Lisa, The mitochondrial permeability transition pore: Molecular nature and role as a target in cardioprotection, *Journal of Molecular and Cellular Cardiology*, 78 (2015) 100-106.
- [8] P. Bernardi, A. Rasola, M. Forte, G. Lippe, The Mitochondrial Permeability Transition Pore: Channel Formation by F-ATP Synthase, Integration in Signal Transduction, and Role in Pathophysiology, *Physiological reviews*, 95 (2015) 1111-1155.

- [9] C. Brenner, M. Moulin, Physiological roles of the permeability transition pore, *Circulation research*, 111 (2012) 1237-1247.
- [10] J.Q. Kwong, J.D. Molkentin, Physiological and pathological roles of the mitochondrial permeability transition pore in the heart, *Cell metabolism*, 21 (2015) 206-214.
- [11] S.S. Smaili, J.T. Russell, Permeability transition pore regulates both mitochondrial membrane potential and agonist-evoked Ca<sup>2+</sup> signals in oligodendrocyte progenitors, *Cell Calcium*, 26 (1999) 121-130.
- [12] J. Henry-Mowatt, C. Dive, J.-C. Martinou, D. James, Role of mitochondrial membrane permeabilization in apoptosis and cancer, *Oncogene*, 23 (2004) 2850-2860.
- [13] S. Javadov, M. Karmazyn, Mitochondrial Permeability Transition Pore Opening as an Endpoint to Initiate Cell Death and as a Putative Target for Cardioprotection, *Cellular Physiology and Biochemistry*, 20 (2007) 1-22.
- [14] G. Kroemer, L. Galluzzi, C. Brenner, Mitochondrial membrane permeabilization in cell death, *Physiological reviews*, 87 (2007) 99-163.
- [15] J.J. Lemasters, A.-L. Nieminen, T. Qian, L.C. Trost, S.P. Elmore, Y. Nishimura, R.A. Crowe, W.E. Cascio, C.A. Bradham, D.A. Brenner, B. Herman, The mitochondrial permeability transition in cell death: a common mechanism in necrosis, apoptosis and autophagy, *Biochimica et Biophysica Acta (BBA) - Bioenergetics*, 1366 (1998) 177-196.
- [16] A.P. Halestrap, P. Pasdois, The role of the mitochondrial permeability transition pore in heart disease, *Biochimica et Biophysica Acta (BBA) - Bioenergetics*, 1787 (2009) 1402-1415.
- [17] S. Javadov, M. Karmazyn, N. Escobales, Mitochondrial Permeability Transition Pore Opening as a Promising Therapeutic Target in Cardiac Diseases, *Journal of Pharmacology and Experimental Therapeutics*, 330 (2009) 670-678.
- [18] J.N. Weiss, P. Korge, H.M. Honda, P. Ping, Role of the Mitochondrial Permeability Transition in Myocardial Disease, *Circulation research*, 93 (2003) 292-301.
- [19] R.J. White, I.J. Reynolds, Mitochondrial depolarization in glutamate-stimulated neurons: an early signal specific to excitotoxin exposure, *The Journal of neuroscience : the official journal of the Society for Neuroscience*, 16 (1996) 5688-5697.
- [20] L.J. Martin, S. Semenkow, A. Hanaford, M. Wong, Mitochondrial permeability transition pore regulates Parkinson's disease development in mutant alpha-synuclein transgenic mice, *Neurobiology of aging*, 35 (2014) 1132-1152.
- [21] M.D. Norenberg, K.V.R. Rao, The mitochondrial permeability transition in neurologic disease, *Neurochemistry International*, 50 (2007) 983-997.
- [22] V. Calabrese, G. Scapagnini, A.M. Giuffrida Stella, T.E. Bates, J.B. Clark, Mitochondrial Involvement in Brain Function and Dysfunction: Relevance to Aging, *Neurodegenerative Disorders and Longevity*, *Neurochem Res*, 26 (2001) 739-764.
- [23] L.J. Martin, B. Gertz, Y. Pan, A.C. Price, J.D. Molkentin, Q. Chang, The mitochondrial permeability transition pore in motor neurons: Involvement in the pathobiology of ALS mice, *Experimental Neurology*, 218 (2009) 333-346.
- [24] A. Rasola, P. Bernardi, The mitochondrial permeability transition pore and its involvement in cell death and in disease pathogenesis, *Apoptosis : an international journal on programmed cell death*, 12 (2007) 815-833.
- [25] A.L. King, T.M. Swain, Z. Mao, U.S. Udoh, C.R. Oliva, A.M. Betancourt, C.E. Griguer, D.R. Crowe, M. Lesort, S.M. Bailey, Involvement of the mitochondrial permeability transition pore in chronic ethanol-mediated liver injury in mice, *American journal of physiology. Gastrointestinal and liver physiology*, 306 (2014) G265-277.
- [26] Y. Masubuchi, C. Suda, T. Horie, Involvement of mitochondrial permeability transition in acetaminophen-induced liver injury in mice, *Journal of hepatology*, 42 (2005) 110-116.

- [27] L. Dalla Via, A.N. Garcia-Argaez, M. Martinez-Vazquez, S. Grancara, P. Martinis, A. Toninello, Mitochondrial permeability transition as target of anticancer drugs, *Current pharmaceutical design*, 20 (2014) 223-244.
- [28] V.K. Rao, E.A. Carlson, S.S. Yan, Mitochondrial permeability transition pore is a potential drug target for neurodegeneration, *Biochimica et biophysica acta*, 1842 (2014) 1267-1272.
- [29] K. Boengler, D. Hilfiker-Kleiner, G. Heusch, R. Schulz, Inhibition of permeability transition pore opening by mitochondrial STAT3 and its role in myocardial ischemia/reperfusion, *Basic research in cardiology*, 105 (2010) 771-785.
- [30] C. Martel, L.H. Huynh, A. Garnier, R. Ventura-Clapier, C. Brenner, Inhibition of the Mitochondrial Permeability Transition for Cytoprotection: Direct versus Indirect Mechanisms, *Biochemistry Research International*, 2012 (2012) 13.
- [31] G. Morciano, C. Giorgi, M. Bonora, S. Punzetti, R. Pavesani, M.R. Wieckowski, G. Campo, P. Pinton, Molecular identity of the mitochondrial permeability transition pore and its role in ischemia-reperfusion injury, *Journal of Molecular and Cellular Cardiology*, 78 (2015) 142-153.
- [32] S. Javadov, A. Kuznetsov, Mitochondrial Permeability Transition and Cell Death: The Role of Cyclophilin D, *Frontiers in physiology*, 4 (2013) 76.
- [33] C.P. Baines, R.A. Kaiser, N.H. Purcell, N.S. Blair, H. Osinska, M.A. Hambleton, E.W. Brunskill, M.R. Sayen, R.A. Gottlieb, G.W. Dorn, J. Robbins, J.D. Molkentin, Loss of cyclophilin D reveals a critical role for mitochondrial permeability transition in cell death, *Nature*, 434 (2005) 658-662.
- [34] R.A. Haworth, D.R. Hunter, The Ca<sup>2+</sup>-induced membrane transition in mitochondria. II. Nature of the Ca<sup>2+</sup> trigger site, *Archives of biochemistry and biophysics*, 195 (1979) 460-467.
- [35] N. Fournier, G. Ducet, A. Crevat, Action of cyclosporine on mitochondrial calcium fluxes, *J Bioenerg Biomembr*, 19 (1987) 297-303.
- [36] M. Crompton, H. Ellinger, A. Costi, Inhibition by cyclosporin A of a Ca<sup>2+</sup>-dependent pore in heart mitochondria activated by inorganic phosphate and oxidative stress, *The Biochemical journal*, 255 (1988) 357-360.
- [37] A. Laupacis, P.A. Keown, R.A. Ulan, N. McKenzie, C.R. Stiller, Cyclosporin A: a powerful immunosuppressant, *Canadian Medical Association Journal*, 126 (1982) 1041-1046.
- [38] P. Bellwon, M. Culot, A. Wilmes, T. Schmidt, M.G. Zurich, L. Schultz, O. Schmal, A. Gramowski-Voss, D.G. Weiss, P. Jennings, A. Bal-Price, E. Testai, W. Dekant, Cyclosporine A kinetics in brain cell cultures and its potential of crossing the blood-brain barrier, *Toxicology in vitro : an international journal published in association with BIBRA*, 30 (2015) 166-175.
- [39] A. Zulian, E. Rizzo, M. Schiavone, E. Palma, F. Tagliavini, B. Blaauw, L. Merlini, N.M. Maraldi, P. Sabatelli, P. Braghetta, P. Bonaldo, F. Argenton, P. Bernardi, NIM811, a cyclophilin inhibitor without immunosuppressive activity, is beneficial in collagen VI congenital muscular dystrophy models, *Human molecular genetics*, 23 (2014) 5353-5363.
- [40] M.J. Hansson, G. Mattiasson, R. Mansson, J. Karlsson, M.F. Keep, P. Waldmeier, U.T. Rugg, J.M. Dumont, K. Besseghir, E. Elmer, The nonimmunosuppressive cyclosporin analogs NIM811 and UNIL025 display nanomolar potencies on permeability transition in brain-derived mitochondria, *J Bioenerg Biomembr*, 36 (2004) 407-413.
- [41] H.-x. Guo, F. Wang, K.-q. Yu, J. Chen, D.-l. Bai, K.-x. Chen, X. Shen, H.-l. Jiang, Novel cyclophilin D inhibitors derived from quinoxaline exhibit highly inhibitory activity against rat mitochondrial swelling and Ca<sup>2+</sup> uptake/release, *Acta Pharmacol Sin*, 26 (2005) 1201-1211.
- [42] S. Murasawa, K. Iuchi, S. Sato, T. Noguchi-Yachide, M. Sodeoka, T. Yokomatsu, K. Dodo, Y. Hashimoto, H. Aoyama, Small-molecular inhibitors of Ca<sup>2+</sup>-induced mitochondrial permeability transition (MPT) derived from muscle relaxant dantrolene, *Bioorganic & Medicinal Chemistry*, 20 (2012) 6384-6393.

- [43] S. Roy, J. Šileikytė, B. Neuenswander, M.P. Hedrick, T.D.Y. Chung, J. Aubé, F.J. Schoenen, M.A. Forte, P. Bernardi, N-Phenylbenzamides as Potent Inhibitors of the Mitochondrial Permeability Transition Pore, *ChemMedChem*, 11 (2016) 283-288.
- [44] Y.S. Kim, S.H. Jung, B.G. Park, M.K. Ko, H.S. Jang, K. Choi, J.H. Baik, J. Lee, J.K. Lee, A.N. Pae, Y.S. Cho, S.J. Min, Synthesis and evaluation of oxime derivatives as modulators for amyloid beta-induced mitochondrial dysfunction, *European journal of medicinal chemistry*, 62 (2013) 71-83.
- [45] S. Jung, K. Choi, A.N. Pae, J.K. Lee, H. Choo, G. Keum, Y.S. Cho, S.J. Min, Facile diverted synthesis of pyrrolidinyl triazoles using organotrifluoroborate: discovery of potential mPTP blockers, *Organic & biomolecular chemistry*, 12 (2014) 9674-9682.
- [46] A. Elkamhawy, J.-e. Park, A.H.E. Hassan, H. Ra, A.N. Pae, J. Lee, B.-G. Park, B. Moon, H.-M. Park, E.J. Roh, Discovery of 1-(3-(benzyloxy)pyridin-2-yl)-3-(2-(piperazin-1-yl)ethyl)urea: A new modulator for amyloid beta-induced mitochondrial dysfunction, *European journal of medicinal chemistry*, 128 (2017) 56-69.
- [47] K. Kajitani, M. Fujihashi, Y. Kobayashi, S. Shimizu, Y. Tsujimoto, K. Miki, Crystal structure of human cyclophilin D in complex with its inhibitor, cyclosporin A at 0.96-Å resolution, *Proteins*, 70 (2008) 1635-1639.
- [48] J.J. Kaminski, J.M. Hilbert, B.N. Pramanik, D.M. Solomon, D.J. Conn, R.K. Rizvi, A.J. Elliott, H. Guzik, R.G. Lovey, Antiulcer agents. 2. Gastric antisecretory, cytoprotective, and metabolic properties of substituted imidazo[1,2-a]pyridines and analogs, *Journal of Medicinal Chemistry*, 30 (1987) 2031-2046.
- [49] D. Liao, L. Sun, W. Liu, S. He, X. Wang, X. Lei, Necrosulfonamide inhibits necroptosis by selectively targeting the mixed lineage kinase domain-like protein, *MedChemComm*, 5 (2014) 333-337.

**Tables****Table 1.** *In vitro* blocking activity of the new ureas against A $\beta$ -induced mPTP opening (JC-1 assay) at a dose of 5  $\mu$ M

Cpd	X	R <sub>1</sub>	R <sub>2</sub>	Increased g/r ratio (%) <sup>a</sup>	Cpd	X	R <sub>1</sub>	R <sub>2</sub>	Increased g/r ratio (%) <sup>a</sup>
<b>7aa</b>	CH	H	2-Fluorophenyl	69	<b>7ef</b>	CH	2-Cl	4-Methylphenyl	22
<b>7ab</b>	CH	H	3-Fluorophenyl	13	<b>7eg</b>	CH	2-Cl	1-Naphthyl	77
<b>7ac</b>	CH	H	3,4-Dichlorophenyl	19	<b>7fa</b>	CH	3-Cl	Phenyl	14
<b>7ba</b>	N	H	2-Fluorophenyl	123	<b>7fb</b>	CH	3-Cl	2-Fluorophenyl	11
<b>7bb</b>	N	H	3-Fluorophenyl	111	<b>7fc</b>	CH	3-Cl	3-Fluorophenyl	13
<b>7ca</b>	CH	3-F	Benzyl	9	<b>7fd</b>	CH	3-Cl	3-Chlorophenyl	55
<b>7cb</b>	CH	3-F	Phenyl	23	<b>7fe</b>	CH	3-Cl	3,4-Dichlorophenyl	10
<b>7cc</b>	CH	3-F	2-Fluorophenyl	23	<b>7ff</b>	CH	3-Cl	4-Methylphenyl	26
<b>7cd</b>	CH	3-F	3-Fluorophenyl	34	<b>7fg</b>	CH	3-Cl	4-Trifluoromethylphenyl	27
<b>7ce</b>	CH	3-F	3,4-Dichlorophenyl	35	<b>7fh</b>	CH	3-Cl	1-Naphthyl	106
<b>7cf</b>	CH	3-F	4-Methylphenyl	22	<b>7ga</b>	CH	4-Cl	2-Fluorophenyl	27
<b>7cg</b>	CH	3-F	4-Trifluoromethylphenyl	23	<b>7gb</b>	CH	4-Cl	3-Fluorophenyl	15
<b>7da</b>	N	3-F	Benzyl	69	<b>7gc</b>	CH	4-Cl	3-Chlorophenyl	46
<b>7db</b>	N	3-F	3-Fluorophenyl	98	<b>7gd</b>	CH	4-Cl	3,4-Dichlorophenyl	47
<b>7dc</b>	N	3-F	3,4-Dichlorophenyl	101	<b>7ge</b>	CH	4-Cl	4-Methylphenyl	44
<b>7dd</b>	N	3-F	4-Methylphenyl	96	<b>7gf</b>	CH	4-Cl	4-Trifluoromethylphenyl	91
<b>7ea</b>	CH	2-Cl	Phenyl	80	<b>7gg</b>	CH	4-Cl	1-Naphthyl	52
<b>7eb</b>	CH	2-Cl	2-Fluorophenyl	38	<b>7ha</b>	CH	4-F	2-Fluorophenyl	27
<b>7ec</b>	CH	2-Cl	3-Fluorophenyl	32	<b>7hb</b>	CH	4-F	3-Fluorophenyl	18
<b>7ed</b>	CH	2-Cl	3-Chlorophenyl	25	<b>7hc</b>	CH	4-F	3-Chlorophenyl	91
<b>7ee</b>	CH	2-Cl	3,4-Dichlorophenyl	36	<b>CsA</b>	–	–	–	46

<sup>a</sup> % Increase of fluorescence-ratio (green/red) after treatment of each compound and A $\beta$  with regard to that of A $\beta$  alone (100%). All data are reported as the average of duplicates.

**Table 2.** Results of evaluation of compounds-induced deterioration of mitochondrial energy production and neuronal cells viability.

Cpd	ATP Production (%) <sup>a</sup>	Viability (%) <sup>b</sup>	Cpd	ATP Production (%) <sup>a</sup>	Viability (%) <sup>b</sup>
<b>7ec</b>	106	86	<b>7fc</b>	99	91
<b>7ed</b>	124	84	<b>7ff</b>	108	95
<b>7ee</b>	123	60	<b>Piracetam</b>	88	ND <sup>c</sup>
<b>7fa</b>	109	98	<b>CsA</b>	ND <sup>c</sup>	90
<b>7fb</b>	104	115			

<sup>a</sup> % ATP production in hippocampal neuronal cell line HT-22 calculated after 7 hours incubation with 5  $\mu$ M of each compound. All data are reported as the average of duplicates.

<sup>b</sup> % MTT-cell viability of hippocampal neuronal cell line HT-22 after 24 hours incubation with at 5  $\mu$ M of each compound. All data are reported as the average of duplicates.

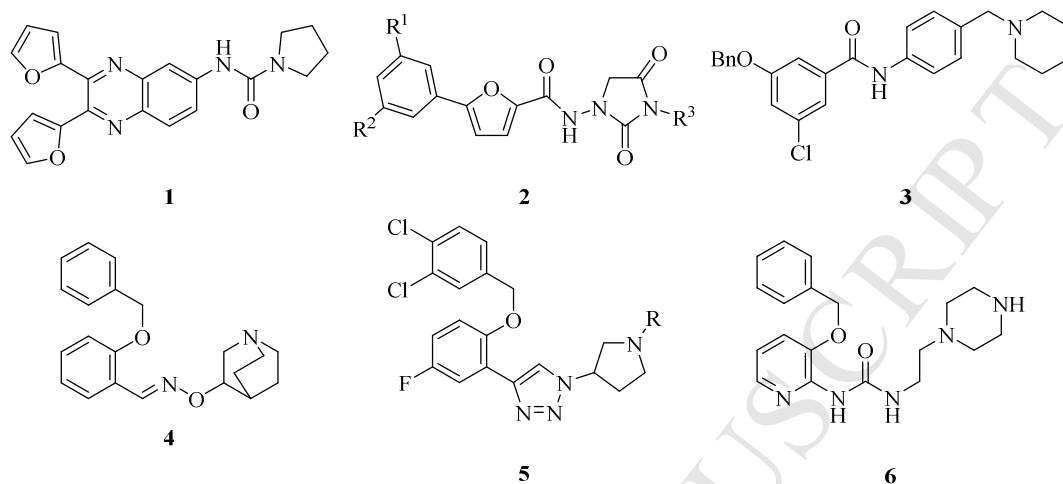
<sup>c</sup> ND not determined.

**Table 3.** Assessment results of protection against A $\beta$ -induced impairment of mitochondrial ATP production and neurocytotoxicity.

Cpd	% of ATP Recovery <sup>a</sup>	% of Inhibition of A $\beta$ -induced cytotoxicity <sup>b</sup>	Cpd	% of ATP Recovery <sup>a</sup>	% of Inhibition of A $\beta$ -induced cytotoxicity <sup>b</sup>
<b>7ec</b>	78	14	<b>7fc</b>	69	38
<b>7ed</b>	91	21	<b>7ff</b>	54	17
<b>7fa</b>	90	31	<b>Piracetam</b>	127	29
<b>7fb</b>	43	67			

<sup>a</sup> % Recovery of ATP production in A $\beta$ -suppressed mitochondrial ATP production within hippocampal neuronal cell line HT-22 after 7 hours incubation with 5  $\mu$ M concentrations of both of A $\beta$  and each tested compound. All data are reported as the average of duplicates.

<sup>b</sup> % A $\beta$ -intoxicated hippocampal HT-22 cells remaining viable after 24 hours incubation with 5  $\mu$ M concentrations of both of A $\beta$  and each tested compound. All data are reported as the average of duplicates.

**Figures and Scheme**

**Fig. 1.** Reported small molecules with CYPs inhibition activity

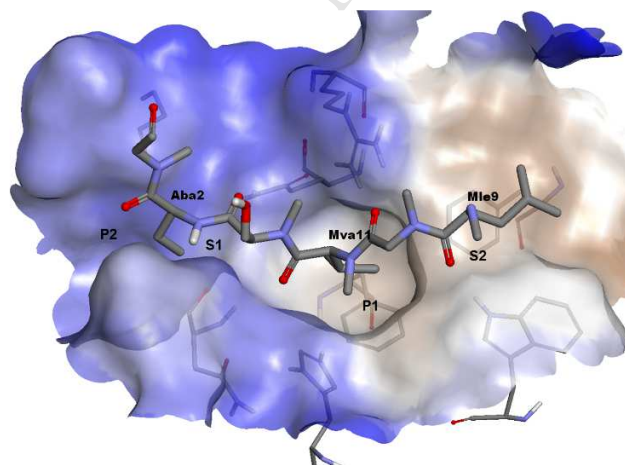


**Fig. 2.** The crystal structure of cyclosporin A (CsA) binding to cyclophilin D (CypD). For clarity of display, non-interacting residues and side chains of CsA are not displayed.

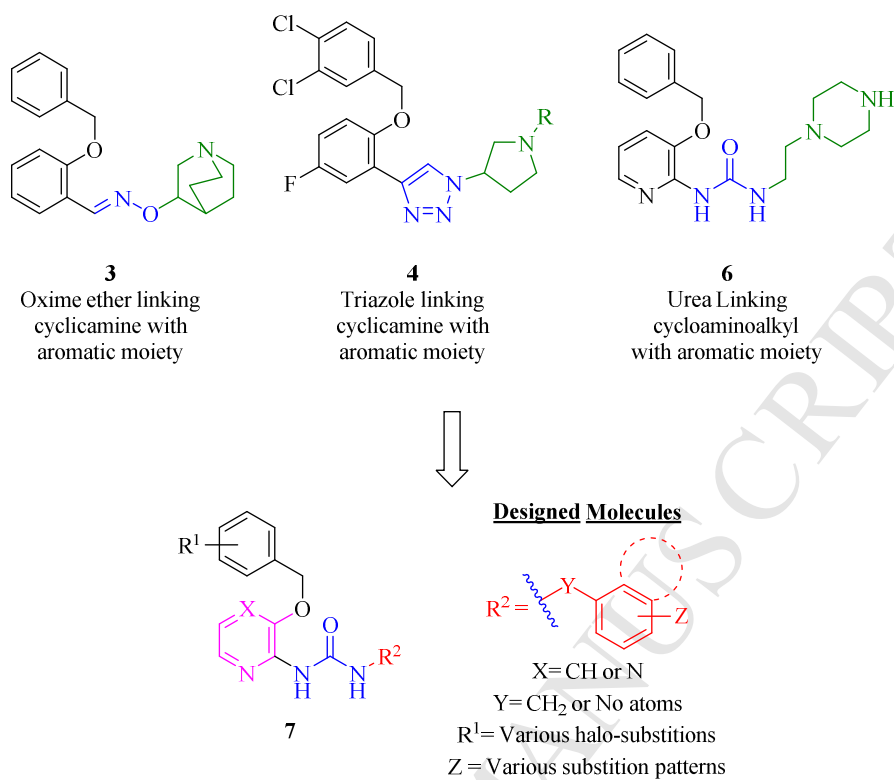
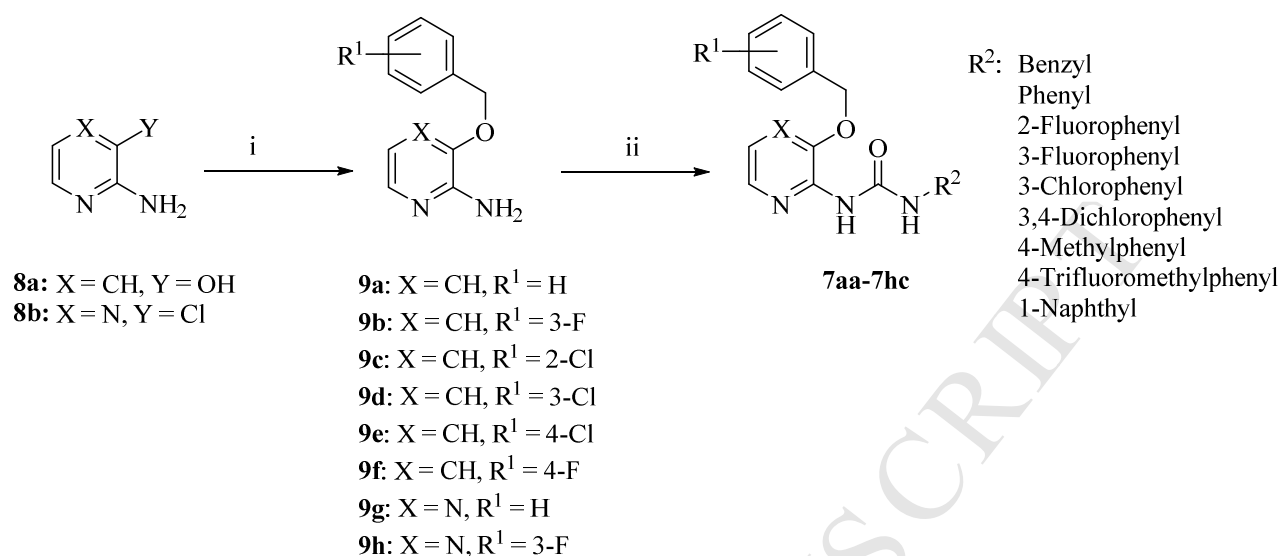


**Fig. 3.** Design of urea derivatives incorporating additional aromatic moieties as mPTP blockers



**Scheme 1.** Reagents and conditions: (i) **9a** was purchased; for **9b–f**: to **8a** starting material, 1) NaOH, H<sub>2</sub>O, Bu<sub>4</sub>NBr, DCM, rt, 15 min, 2) appropriate benzyl bromide, DCM, rt, 18 h; for **9g** and **9h**: to **8b** starting material, NaH (60% in mineral oil), appropriate benzyl alcohol derivative, DMF, 100 °C, 15 h (ii) appropriate isocyanate derivative, THF, reflux, 3–6 h.

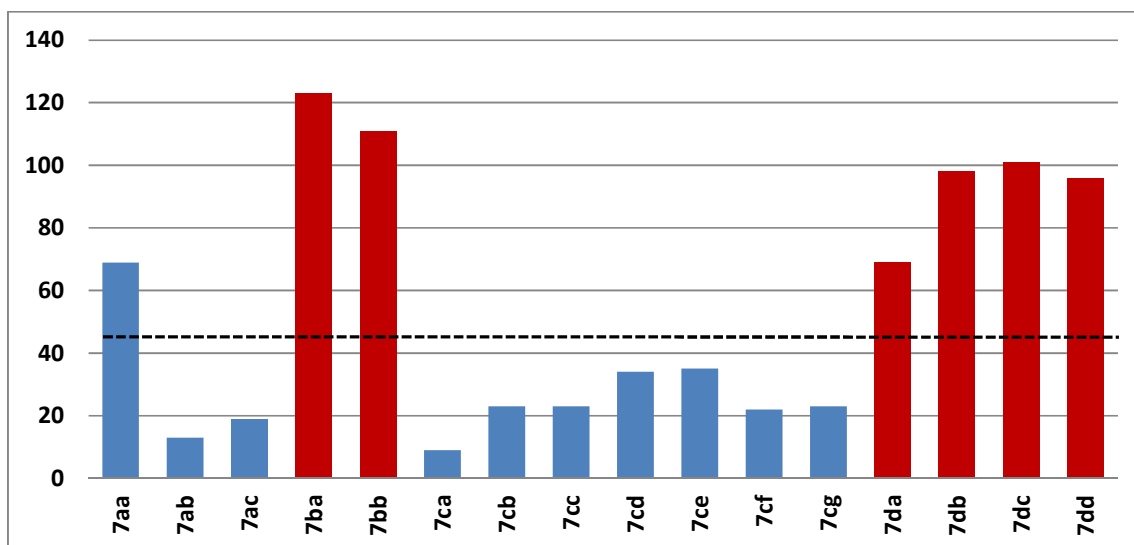


**Fig. 4.** Percentage increase in the fluorescence ratio (green/red) after treatment with pyridyl derivatives (blue) or pyrazinyl derivatives (red) and A $\beta$  with respect to that of A $\beta$  alone (100%). Dashed line represent fluorescence ratio of cyclosporin A (CsA) used as a control.

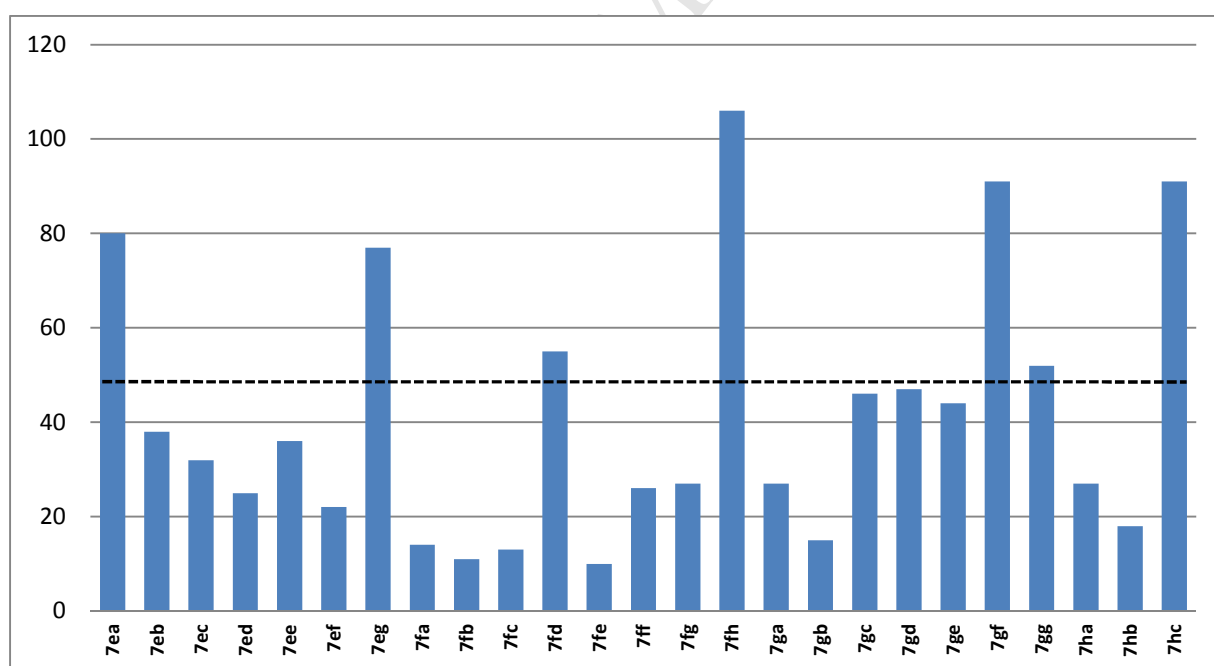


**Fig. 5.** Percentage increase in the fluorescence ratio (green/red) after treatment with pyridyl derivatives (7ea–7hc) and A $\beta$  with respect to that of A $\beta$  alone (100%). Dashed line represent fluorescence ratio of cyclosporin A (CsA) used as a control.

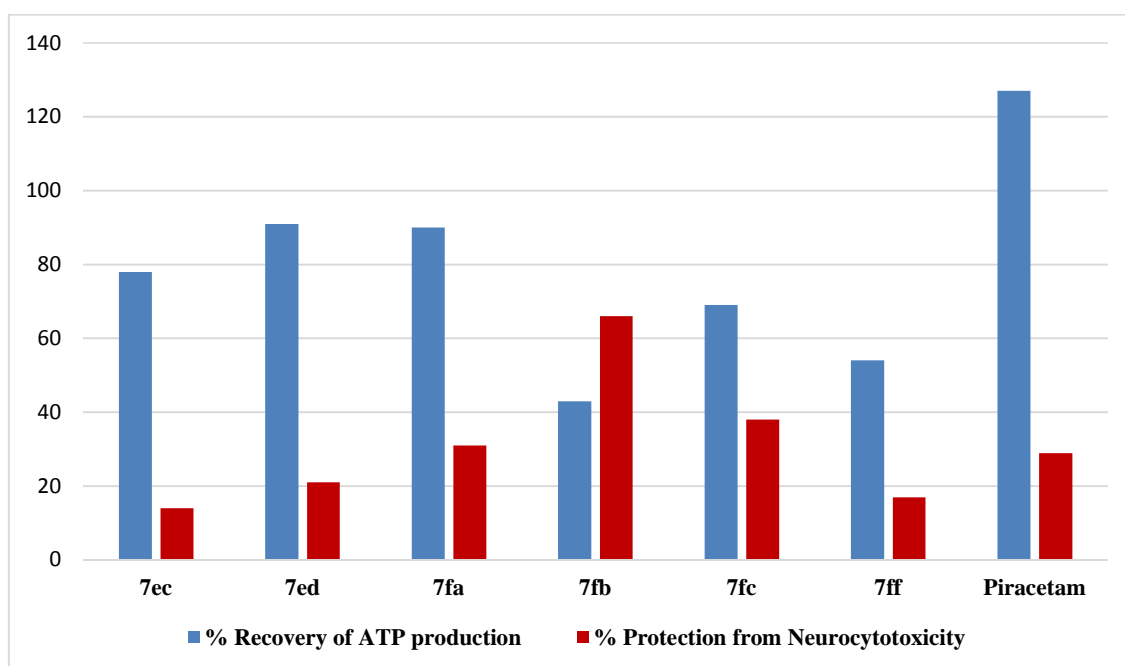


**Fig. 6.** The percentage of protective effect elicited by 5  $\mu\text{M}$  concentration of each tested compound from impairment of ATP production and neurocytotoxicity induced by a 5  $\mu\text{M}$  concentration of  $\text{A}\beta$ .

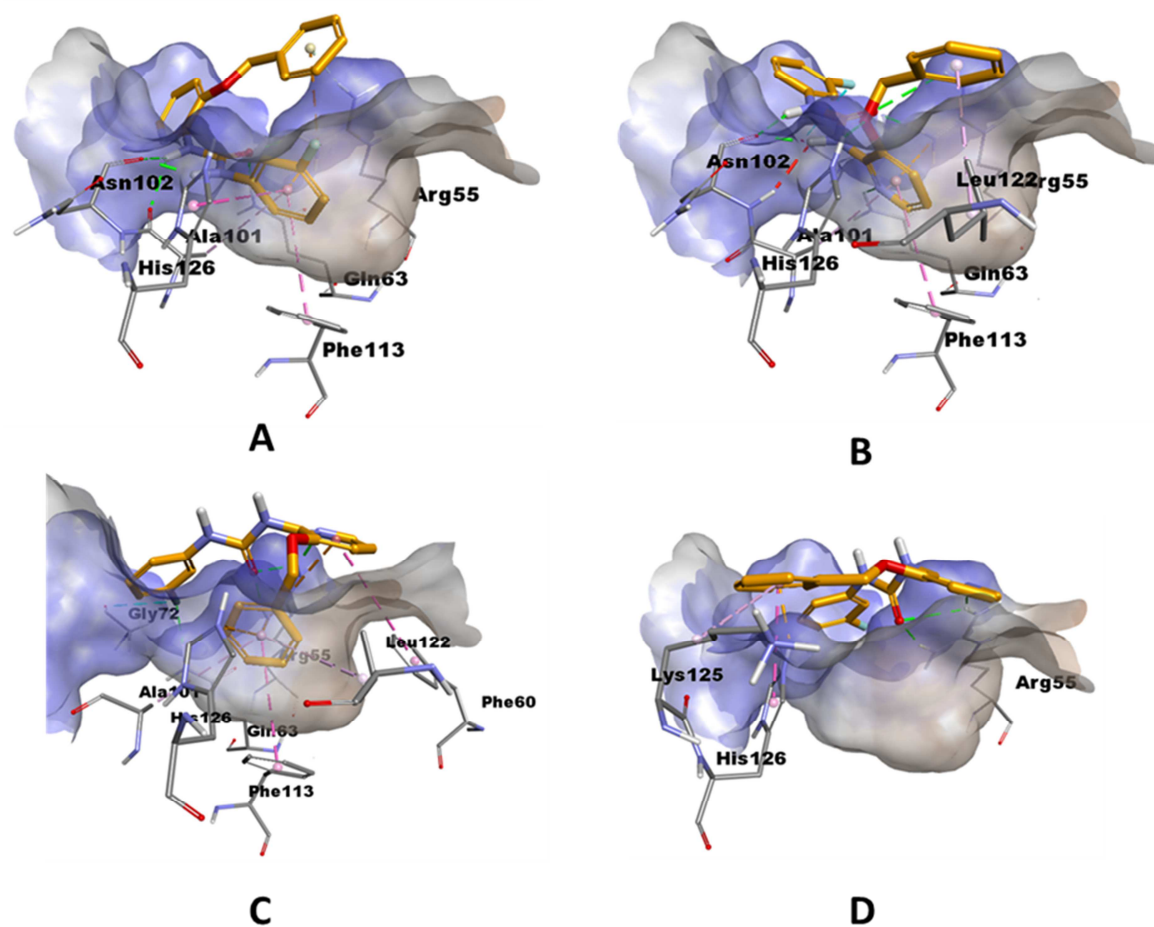


**Fig. 7.** Different Binding modes of compound **7ab**; A) Binding mode 1 subtype 1; in which the eastern aromatic moiety docks into the hydrophobic pocket 1. B) Binding mode 1 subtype 2; in which the pyridine ring docks into the hydrophobic pocket 1. C) Binding mode 1 subtype 3; in which the aromatic ring of the benzyloxy moiety docks into the hydrophobic pocket 1. D) Binding mode 2; in which the hydrophobic pocket 1 is vacant while compound **7ab** is docked above it.

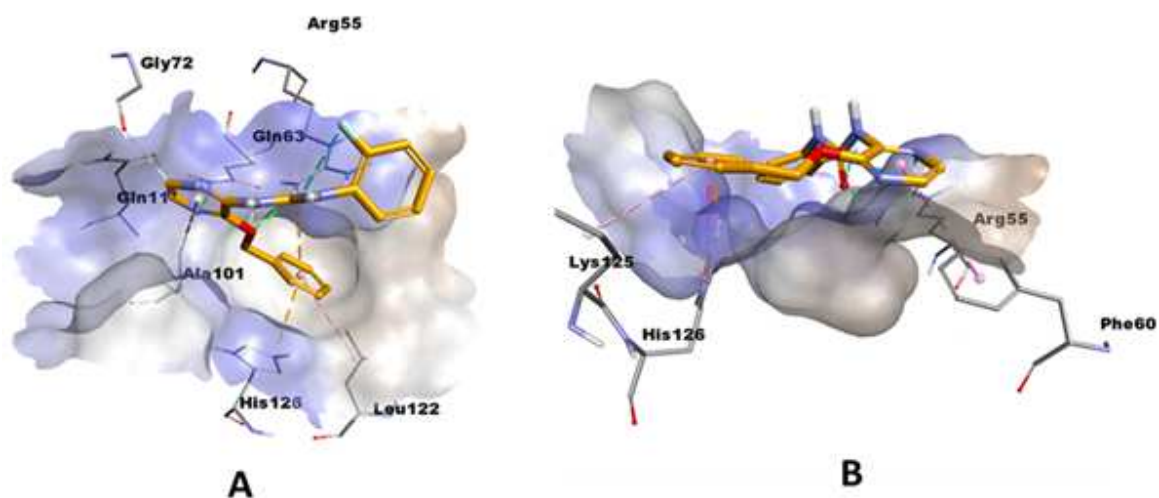


**Fig. 8.** The most favorable binding modes of selected inefficient mPTP blocker; A) Compound **7ba** showing binding mode 1 subtype 3; in which the aromatic ring of the benzyloxy moiety docks into the hydrophobic pocket 1. B) Compound **7ba** showing binding mode 2; in which the hydrophobic pocket 1 is vacant while compound **7ba** is docked above it.

**Research Highlights**

- Forty one pyridyl urea derivatives have been synthesized as potential mPTP blockers.
- The inhibitory activity of twenty five compounds against A $\beta$ -induced mPTP opening was superior to that of the standard Cyclosporin A (CsA).
- **7fb** has been identified as a lead compound protecting neuronal cells against 67% of neurocytotoxicity and 43% of suppression of mitochondrial ATP production.
- A molecular docking model presented a plausible binding mode for the target compounds with cyclophilin D (CypD) receptor as a major component of mPTP.